1 **Running head**: Utility of root cortical cell size under drought

2 **Corresponding author**:

3 Jonathan P. Lynch, Department of Plant Science, The Pennsylvania State University, University
4 Park, PA, USA 16802, 814-863-2256, jpl4@psu.edu

5 **Journal research area:** Ecophysiology and sustainability

6

7

8

9 **Large root cortical cell size improves drought tolerance in maize (*Zea mays L.*)**

10 **Joseph G. Chimungu, Kathleen M. Brown, Jonathan P. Lynch***

11 **Summary**: Large cortical cells substantially reduce root respiration, permitting greater root

12 growth and exploration of deep soil, thereby improving water acquisition, plant growth, and yield

13 under drought.

14

This research was supported by the National Science Foundation/Basic Research to Enhance Agricultural Development (grant number: 4184–UM–NSF–5380) and Agriculture and Food Research Initiative competitive grant number: 2014-67013-2157 of the USDA National Institute of Food and Agriculture.

Department of Plant Science, The Pennsylvania State University, University Park, PA, USA 16802

Abstract

The objective of this study was to test the hypothesis that large cortical cell size would improve drought tolerance by reducing root metabolic costs. Maize lines contrasting in root cortical cell size (CCS) measured as cross-sectional area were grown under well-watered and water-stressed conditions in greenhouse mesocosms and in the field in the USA and in Malawi. CCS varied among genotypes, ranging from 101 to 533 μm^2.In mesocosms large CCS reduced respiration per unit root length by 59%.Under water stress in mesocosms, lines with large CCS had between 21% and 27% deeper rooting (D_{95}), 50% greater stomatal conductance, 59% greater leaf CO_2 assimilation, and between34% and44% greater shoot biomass than lines with small CCS. Under water stress in the field, lines with large CCS had between 32% and 41%deeper rooting (D_{95}), 32% lighter stem water $\delta^{18}O$ signature signifying deeper water capture, between 22%and30% greater leaf relative water content, between 51% and 100% greater shoot biomass at flowering, and between 99% and 145% greater yield than lines with small cells. Our results are consistent with the hypothesis that large CCS improves drought tolerance by reducing the metabolic cost of soil exploration, enabling deeper soil exploration, greater water acquisition, and improved growth and yield under water stress. These results coupled with the substantial genetic variation for CCS in diverse maize germplasm suggest that CCS merits attention as a potential breeding target to improve the drought tolerance of maize and possibly other cereal crops.

Key words: Cortical cell size, root costs, *Zea mays* L., (Maize), drought

Introduction

Suboptimal water availability is a primary constraint for terrestrial plants, and a primary limitation to crop production. In developing countries the problem of yield loss due to drought is most severe (Edmeades, 2008; St.Clair and Lynch, 2010; Edmeades, 2013), the problem will further exacerbated in the future due to climate change (Burke et al., 2009; Schlenker and Lobell, 2010; Lobell et al., 2011a; IPCC, 2014). The development of drought tolerant crops is therefore an important goal for global agriculture. Breeding for drought adaptation using yield as a selection criterion is generally not efficient, since yield is an integration of complex mechanisms at different levels of organization affected by many elements of the phenotype and the environment interacting in complex and often unknown ways. Trait-based selection or ideotype breeding is generally a more efficient selection strategy, permitting the identification of useful sources of variation among lines that have poor agronomic adaptation, elucidation of genotype by environment interactions, and informed trait stacking (Lynch, 2007; Araus et al., 2008; Richards et al., 2010; Wasson et al., 2012; York et al., 2013).

Under drought stress, plants allocate more resources to root growth relative to shoot growth, which can enhance water acquisition (Sharp and Davies, 1979; Palta and Gregory, 1997; Lynch and Ho, 2005).The metabolic costs of soil exploration by root systems are significant, and can exceed 50% of daily photosynthesis (Lambers et al., 2002).With a large root system, each unit of leaf area has more non-photosynthetic tissue to sustain, which may reduce productivity by diverting resources from shoot and reproductive growth (Smucker, 1993; Nielsen et al., 2001; Boyer and Westgate, 2004). Genotypes with less costly root tissue could develop the extensive, deep root systems required to fully utilize soil water resources in drying soil without as much yield penalty. Therefore, root phenes that reduce the metabolic costs of soil exploration, thereby improving water acquisition are likely to be valuable for improving drought tolerance (Lynch and Ho, 2005; Zhu et al., 2010; Lynch, 2011; Richardson et al., 2011; Jaramillo et al., 2013).

Maize (*Zea mays* L.) is the principal global cereal. Maize production is facing major challenges as a result of the increasing frequency and intensity of drought (Tuberosa and Salvi, 2006) and this problem will likely be exacerbated by climate change (Lobell et al., 2011b). The 'steep, cheap and deep' ideotype has been proposed for improving water and nitrogen acquisition by maize when these resources are limited (Lynch, 2013). This ideotype consists of root architectural, anatomical, and physiological traits that may increase rooting depth and thereby improve water acquisition from drying soils. Anatomical phenes could influence the metabolic cost of soil exploration by changing the proportion of respiring and non-respiring root tissue, and affecting the metabolic cost of tissue construction and maintenance, which is an important limitation to root growth and plant development under edaphic stress. Specific anatomical phenes that may contribute to rooting depth by reducing root metabolic costs include components of living cortical area (LCA) (Jaramillo et al., 2013), including root cortical aerenchyma (RCA), cortical cell size (CCS) and cortical cell file number (CCFN; Lynch, 2013).

RCA are large air-filled lacunae which replace living cortical cells as a result of programmed cell death (Evans, 2004). Previous studies have demonstrated that RCA improves crop adaptation to edaphic stress by reducing the metabolic cost of soil exploration and exploitation (Fan et al., 2003; Zhu et al., 2010; Postma and Lynch, 2011a, Saengwilai et al., 2014). RCA is associated with a disproportionate reduction of root respiration, thereby permitting greater root growth and acquisition of soil resources(Fan et al., 2003; Zhu et al., 2010). *SimRoot* modeling indicated that

RCA can substantially increase the acquisition of nitrogen, phosphorus and potassium of maize by reducing respiration and the nutrient content of root tissue (Postma and Lynch, 2011b). Under water stress in the field, maize genotypes with more RCA had deeper roots, better leaf water status, and 800% greater yield than genotypes with less RCA (Zhu et al., 2010). Under N stress in the field and in greenhouse mesocosms, maize genotypes with more RCA had greater rooting depth, greater N capture from deep soil strata, greater N content, greater leaf photosynthesis, greater biomass, and greater yield (Saengwilai et al., 2014a).

LCA refers to the living portion of the cortex that remains after the formation of aerenchyma (Jaramillo et al., 2013). Recently we have reported that LCA is an important determinant of root metabolic cost and a better predictor of root respiration than RCA (Jaramillo et al., 2013). In that study maize lines contrasting in LCA were grown under well-watered or water-stressed conditions in soil mesocosms, and LCA was associated with reduction of specific root respiration. These results provided the impetus to investigate the relative contribution of each component of LCA to metabolic cost. Our focus here is on root cortical cell size (CCS).

Plant cell size varies substantially, both among and within species (Sugimoto-Shirasu and Roberts, 2003). Cell size in a given species and tissue is under genetic control and results from the coordinated control of cell growth and cell division (Sablowski and Carnier Dornelas, 2013).The increased volume of individual cells is attributable to cytoplasmic growth and cell expansion (Marshall et al., 2012; Chevalier et al., 2013). Cytoplasmic growth is the net accumulation of macromolecules and cellular organelles, while cell expansion refers to increased cell volume caused by enlargement of the vacuole (Taiz, 1992; Sablowski and Carnier Dornelas, 2013). Lynch (2013) proposed that large cortical cell size would decrease the metabolic costs of root growth and maintenance, both in terms of the carbon cost of root respiration as well as the nutrient content of living tissue, by increasing the ratio of vacuolar to cytoplasmic volume.

The objective of this study was to test the hypothesis that large cortical cell size would reduce specific root respiration (i.e., respiration per unit root length), which under water stress would result in greater root growth, greater acquisition of subsoil water, better plant water status, and improved plant growth and yield. Diverse sets of genotypes (including landraces and recombinant inbred lines) contrasting for CCS were evaluated under water stress and well watered conditions in soil mesocosms in controlled environments, in the field in the USA using automated rainout shelters, and in the field in Malawi. Our results demonstrate that substantial variation for CCS exists in maize and that this variation has substantial effects on the metabolic cost of soil exploration and thereby water acquisition under drought.

RESULTS

Substantial variation for CCS exists in maize

We observed substantial variation for CCS in maize (Fig. 1, Supplemental table S1). Cell sizes vary across the root cortex, being greatest in the center of the cortex (mid-cortical band) and decreasing in size towards the epidermis (outer band) and endodermis (inner band)(Table 1).Cell size in the mid-cortical band was correlated with size of cells in the outer band ($r = 0.75$, $p<0.05$) and inner band ($r = 0.45$, $p<0.05$).In this study the median cell size for the mid-cortical region was chosen as a representative value for the root CCS. There was over 3-fold variation for CCS among Malawian landraces in MW2012-1, with the largest cells having a cross-sectional area of

533 μm^2 and smallest cells 151μm^2 (supplemental Table S1). Among RILs in greenhouse experiment I (GH1), variation for CCS was over 5-fold (101$\mu m^2$to 514μm^2) (supplemental Table S1). Cortical cell diameter was weakly correlated with cell length (Supplemental figure S2).

To describe the pattern of cell size variation among various tissues, we measured the size of parenchyma cells in the leaf mid-rib, mesocotyl cortex and primary root cortex. Generally the cells were larger in the leaf midrib and mesocotyl compared to the root cortex (Supplemental Fig. S1). Cell size variation in the root cortex was correlated with size variation in the mesocotyl cortex (r=0.54, $p<0.01$) and leaf midrib (r=0.40, $p<0.01$). The relationship between mesocotyl and leaf midrib cell size was weak and not significant (r=0.21, ns).

The correlation between the CCS of second nodal crown roots in well-watered and water-stressed was positive and significant in PA2011 (r=0.83, $p<0.05$), PA2012 (r=0.94, $p<0.05$), and MW2012-1 (r=0.79).However, the cells were relatively larger in well-watered compared to water stressed conditions. Trait stability across environments was estimated as the correlation coefficient between CCS measured on young plants in soil mesocosms (30 days after planting, GH2) and mature plants in the field (70 days after planting, PA2011). A positive correlation was found between CCS in mesocosms (GH2) and in the field (PA2011) (r = 0.59, $p<0.05$).

The selected RILs in experiments GH2, GH3, PA2011, PA2012 and MW2012-2 did not show consistent variation in other root phenes; root cortical cell file number, total cortical area, RCA and root diameter (supplemental Table S2& S3). No significant correlations were observed between CCS with either LCA(r = 0.12, $p>0.353$) or RCA (r = 0.004, $p>0.945$)in GH1.

Large CCS is associated with reduced root respiration, greater root growth and better plant water status under drought in mesocosms and in the field

The respiration rate of root segments was measured in plants grown in soil mesocosms in a greenhouse in three experiments(GH1, 2, 3).Large CCS was associated with substantial reduction of specific root respiration; increasing CCS from 100 to 500 um^2 approximately halved root respiration (Fig.2).

In the mesocosms, water stress significantly reduced rooting depth (D_{95}) 30 days after planting in GH2 and GH3 (Table 1, Fig. 3). Under water stress, lines with large CCS correlated with 21% (GH2) and 27% (GH3) deeper rooting depth (D_{95}) than lines with small CCS, and there was no relationship in well-watered conditions (Fig.3, Supplemental figure S3).Water stress in GH3 reduced stomatal conductance by 68% and leaf CO_2 assimilation by 43% at 30 days after planting (Table 1; Fig.4). Under water stress, lines with large CCS had 50% greater stomatal conductance and 59% greater leaf CO_2 assimilation than lines with small CCS (Fig.4).

In the field at Rock Springs, PA, under water stress lines with large CCS had 41% (PA2011) and 32% (PA2012) greater rooting depth (D_{95}), and 22% (PA2011) and 30% (PA2012) greater leaf relative water content than lines with small CCS (Fig. 5, 6 A & B, Supplemental figure S4, Table 2). D_{95} is the depth above which 95% of total root length is located in the soil profile. In the field in Malawi, lines with large CCS had 20% greater leaf relative water content (MW2012-2) (Fig 6C). In addition, genotypes with deeper D_{95} had greater leaf water status than genotypes with shallow D_{95}, while there was no relationship in well watered conditions (PA2011).

Lines with large CCS had lighter stem water $\delta^{18}O$ and greater reliance on deep soil water under water stress in the field

Soil water$\delta^{18}O$ was significantly more enriched in the upper 20 cm of the soil profile and progressively lighter isotopic signature with increasing depth (Fig 7). However, the majority of change in this signature was in the topsoil: 0-10 and 10-20 cm depth (approximately 2.09‰). The soil water $\delta^{18}O$ signatures below 30 cm depth showed no significant difference with depth (Fig 7) and were aggregated as 'deep water'. The stem water$\delta^{18}O$ signatures ranged from -8.9 to -6.2‰ (Table 3). Lines with large CCS had collectively 32% lighter $\delta^{18}O$ signature than that of lines with small CCS (Table 3). Isosource isotopic mixing model was used to determine the proportional contribution of different soil layers (i.e. 10, 20 cm and deep water) to plant water uptake. Lines with large CCS had greater average reliance on 'deep water' and were less reliant on shallow water from the top two soil layers than lines with small CCS (Table 3).

Large CCS was associated with greater plant growth and yield under water stress

In the mesocosms, water stress reduced shoot biomass by 42% in GH2 and 46% in GH3 (Table 1 and Fig.8). Under water stress, lines with large CCS had 80% (GH2)and 83% (GH3)greater shoot biomass than lines with small CCS at 30 days after planting (Table 1and Fig.8).In the field, water stress reduced shoot biomass 46% (PA2011), 38% (PA2012) and 53% (MW2012-2) at70 days after planting (Table 3 and Fig.9). Under water stress in the field, lines with large CCS had greater shoot biomass than lines with small CCS by 51% (PA2011), 81% (PA2012) and 100% (MW2012-2). However, CCS was not associated with biomass in well-watered conditions (Fig.9). Water stress reduced grain yield by 47%PA2012 and 46% MW2012 (Table 2, Fig. 10). Under water stress lines with large CCS had greater grain yield than lines with small CCS by 145% (PA2012) and by 99% (MW2012-2) CCS (Fig.10).

DISCUSSION

Our results support the hypothesis that large CCS increases drought tolerance by reducing root metabolic costs, permitting greater root growth and water acquisition. In the soil mesocosms large CCS was correlated with substantial reduction of root respiration per unit root length. Under water stress, lines with large CCS had deeper rooting, greater stomatal conductance and leaf CO_2 assimilation, and greater shoot biomass than lines with small CCS. Under water stress conditions in rainout shelters in the USA and in the field in Malawi, lines with large CCS had greater root depth, greater exploitation of water from deep soil strata, greater leaf relative water content, and substantially greater grain yield than lines with small CCS.

We observed substantial variation for CCS among diverse maize genotypes, including landraces and recombinant inbred lines. Among recombinant inbred lines variation was approximately 5-fold. In contrast, 3-fold variation was observed within selected landraces collected across Malawi (Supplemental Table 1). The greatest variation for CCS occurs within the mid-cortical band (Supplemental Table 1). In contrast, outer and inner bands had smaller levels of variation within a population (Supplemental Table 1).The reduced variation and smaller cells in outer and inner bands could be related to their functions: the inner band represents highly specialized cells with important functions for the regulation of radial transport in the roots; the outer band provides protection against pathogen entry and in addition the multiseriate epidermal band cells have been associated with root mechanical strength (Striker et al., 2007).Root CCS was correlated with the

size of cells of the mesocotyl cortex and leaf mid-rib parenchyma. We also found excellent correlation between CCS measured in water stressed plants and well-watered plants in the field (Supplemental Fig. S5), although the cells were relatively larger in well-watered compared with water-stressed conditions. We also found good correlation of CCS variation between greenhouse mesocosms and field plants. We conclude that phenotypic screening of large numbers of maize genotypes can be conducted effectively in the greenhouse with young plants, which is considerably faster and cheaper than in the field.

Larger CCS was correlated with substantial reductions in specific root respiration (Fig.2). We propose that as cell size increases, the thickness of the cytoplasm between the plasma membrane and tonoplast is maintained, so that cell enlargement is mostly due to vacuolar enlargement. Increased vacuolar volume relative to cytoplasm may reduce respiration because metabolic activity is greater in the cytoplasm than in the vacuole.

Our results demonstrate that metabolically efficient roots reduce the effects of drought, by permitting access to deep soil water (Fig 3 & 5, Supplemental figure S3 & S4). Rooting depth was positively correlated to CCS under water stress, while there was no relationship in well-watered conditions (Fig.3and 5). These results suggest that the benefit of reduced metabolic demand for root growth is particularly important under water stress. We interpret the large magnitude of this effect as evidence of an autocatalytic effect, whereby incrementally greater root growth leads to better water acquisition, which positively reinforces root growth via greater shoot C gain (Fig 4 A).Indeed, lines with large CCS had greater stomatal conductance and leaf CO2 assimilation in mesocosms (Fig.4 B) and greater RWC in the field than lines with small CCS under water stress, which was directly related to rooting depth (Figs.S5, 3,4,5, and 6).

An additional benefit of reduced root costs could be reduced competition for photosynthates among competing sinks, including developing seeds. In maize, yield losses due to drought are related to carbohydrate availability during the reproductive phase (Boyer and Westgate, 2004). It is difficult to distinguish this indirect benefit of large CCS for yield from the more direct benefit of CCS for root growth and soil exploration, because of the tightly coupled integration of water stress effects on photosynthesis, reproduction, and source-sink relationships. Structural-functional plant modeling (SFPM) may provide useful insights in this context by allowing the quantification and independent manipulation of resource allocation among competing plant sinks. The SFPM *SimRoot* has provided such insights in the context of the effects of RCA on internal resource allocation in maize (Postma 2011a,b). However, *SimRoot* is not currently parameterized for reproductive growth.

The $\delta^{18}O$ signature in soil water is used as a natural tracer for water sources captured from the soil, because no isotopic fractionation occurs during water uptake and transport (Ehleringer and Dawson, 1992; Dawson and Pate, 1996; Ehleringer et al., 2000). We used natural variation in the $\delta^{18}O$ signature of soil water in the profile to provide insight into the potential link between root depth and water acquisition (Fig 4, 5, 6, & 7). The net effect of evaporation is an enrichment of heavy isotopes in the topsoil. In the subsoil, the isotope signature is attributed to the combination of the evaporation effect and the isotopic signatures of irrigation water and rainfall, resulting in a gradient of $\delta^{18}O$ with soil depth (Fig. 6). In this study we hypothesized that large CCS improves drought tolerance in maize by reducing the metabolic cost of soil exploration, enabling deeper soil exploration and greater water acquisition. Stem water $\delta^{18}O$ signatures showed that lines with large

CCS had 32% lighter isotope signatures and greater dependency on deep soil water than lines with small CCS (Table 3). The difference in stem water δ^{18}Obetween lines with large CCS and small CCS could be attributed to their differences in rooting depth (Fig 3 & 5).

We found that large root CCS was associated with large cell size of parenchyma in the leaf mid-rib, and we anticipate this relationship also holds with other parenchyma cells in the leaf. Large leaf cells might influence the metabolic efficiency for light capture per unit volume, by analogy with our hypothesis that large root cortical cells reduce the metabolic cost of capturing soil resources. However, the relationship between cell size and photosynthesis remains unresolved, as illustrated by the contradictory hypotheses put forward by several authors. A negative correlation between photosynthesis and mesophyll cell size in several species was reported by (El-Sharkawy and Hesketh, 1965; Wilson and Cooper, 1970; El-sharkawy, 2009), attributed to the increase in cell surface area per volume with reducing cell size, but (Dornhoff and Shibles, 1976) observed no correlation between photosynthesis and cell size in soybean. In contrast, (Warner et al., 1987; Warner and Edwards, 1988; Warner and Edwards, 1989) argued that large cells have greater photosynthetic capacity than smaller cells. Thus, our understanding of the relationship between cell size and photosynthesis is still rudimentary and merits further research. It is noteworthy that in the present study we found that lines with large root CCS had greater photosynthetic rate than lines with small CCS under water stress, while there were no differences in well-watered conditions (Fig 4A).

We attempted to employ 'near isophenic' RILs with common root phenotypes other than CCS (Supplemental table S2 & S3) to evaluate the utility of CCS under water limited conditions. 'Near isophenic' RILs permit the analysis of the physiological effects of variation in CCS while holding other aspects of the plant phenotype as constant as possible to minimize the cofounding effects of other root phenes. Therefore, differences in growth between large CCS and small CCS are most readily explained by variation of CCS rather than by other root anatomical differences. In addition we found that there was no correlation between CCS and RCA. These results are consistent with other studies. Burton et al., (2013) working with a large population of Zea species reported RCA was not correlated to any of anatomical phene. Genotypic variation for CCS was not associated with genotypic variation for other obvious features of the plant phenotypes observed in nonstressed plots other than those reported here.

In many low input agricultural systems, drought and low soil fertility are primary constraints to crop production. We anticipate that large CCS may have special utility in low-input systems for increasing the acquisition of deep soil resources like nitrate and water, particularly in leaching environments. The utility of CCS for increasing the acquisition of these deep soil resources may interact with other root phenes such as steep root angles (Lynch, 2013; York et al. 2013).

Optimum plant density is a key consideration for maximizing maize grain yield (Cox and Cherney, 2012; Reeves and Cox, 2013). In this study, all field trials were planted at the same standard density of 53000 plants ha^{-1} while in the greenhouse one plant was planted per mesocosm. The fact that our results in mesocosms and two field environments agree with each other is evidence that plant density did not affect the utility of CCS in conditions used in this study. However, in low-input systems, many farmers plant maize at lower densities than used in this study and also intercrop maize with other crops. In contrast, in high-input systems economically optimum plant densities for maize are between 74,000 and 89,000 plants ha^{-1}

(Nielsen, 2012).The influence of CCS on plant performance under low or high densities is unknown. This could possibly be addressed using modelling approaches considering the large number of parameters that will may affect this relationship, including other anatomical and architectural features of the root phenotype and varying soil conditions, N regimes, and precipitation patterns.

Drought and mechanical impedance are two stressors that commonly co-occur in agroecosystems and have a potential to 'overlap' in their impacts on plant growth, consequently affecting the utility of the trait in a particular environment. Small cells have a greater density of cell walls per volume, providing rigidity and strength, and are thus more resistant to buckling and deflection than large cells (Weijschedé et al., 2008). This is particularly important for root penetration in hard soil, which is common under drought. On the other hand, as demonstrated in this study, large cells are important in reducing metabolic cost for soil exploration permitting root growth into deeper soil domains thereby enhancing water acquisition under drought. In addition, large CCS may also interact with other phenes that enhance root penetration in hard soils such as root diameter and root hairs, and may synergistically enhance root penetration under combined stress of drought and mechanical impedance. In this context it is noteworthy that we observed benefits to large CCS whether plants were grown in soil mesocosms, a silt loam soil in the USA, or a sandy clay loam soil in Malawi. These potential tradeoffs and synergisms should be understood better to guide crop breeding programs.

These results add to a growing body of evidence that phenes and phenes states that reduce the metabolic costs of soil exploration improve the capture of limiting soil resources (Lynch and Ho, 2005; Lynch, 2014; Lynch et al., 2014). Such phenes include production of an optimal number of root axes, biomass allocation to metabolically efficient root classes, and reduced tissue respiration (Miller et al., 2003; Jaramillo et al., 2013; Lynch, 2014; Saengwilai et al., 2014b). CCS is an example of an anatomical phene that affects the metabolic costs of soil exploration by affecting tissue respiration. Root cortical aerenchyma (RCA) also affects tissue respiration by converting living cortical cells to air spaces through programmed cell death. Maize genotypes with high RCA formation have reduced root respiration, greater rooting depth, greater water acquisition under drought (Zhu et al., 2010), and greater N acquisition under N limitation (Saengwilai et al., 2014a). Similarly, maize genotypes with reduced cortical cell file number (CCFN) have less root respiration, greater rooting depth, and greater water acquisition under drought (Chimungu et al., 2014). The deployment of root phenotypes with greater metabolic efficiency of soil exploration represents a novel, unexploited paradigm to develop crops with greater resource efficiency and resilience (Lynch, 2014).

Conclusion

Our results demonstrate that large CCS improves drought tolerance in maize by reducing the metabolic costs of soil exploration. Large CCS substantially reduces root respiration. Under water stress lines with large CCS had deeper roots, better exploitation of deep soil water, greater plant water status, greater leaf photosynthesis, and greater shoot biomass and grain yield than lines with small CCS. Our results are entirely supportive of the hypothesis that large CCS reduces the metabolic costs of soil exploration, leading to greater water acquisition in drying soil (Lynch 2013).There is substantial variation for CCS in maize that can be exploited for crop improvement. We suggest that large CCS may have broad relevance in graminaceous crop species lacking

secondary root growth, including rice (*Oryza sativa*), wheat (*Triticumaestivum* L.), barley (*Hordeumvulgare* L.), oats (*Avena sativa*), sorghum (*Sorghum bicolor*), millet (*Pennisetumglaucum*) etc. Large CCS may also be useful for N capture in leaching environments. Although potential fitness tradeoffs for large CCS are not known, it is noteworthy that we observed substantial benefits to large CCS whether plants were grown in soil mesocosms, a silt loam soil in the USA, or a sandy clay loam soil in Malawi.

MATERIALS AND METHODS

Plant materials

Based on preliminary experiments conducted under optimal conditions in the field and greenhouse, a set of 16 IBM lines (Supplemental Table S2) was used to assess the impact of phenotypic variation of CCS on root respiration (GH1). A set of six IBM lines contrasting in CCS was selected for GH2 and PA2011 experiments and another set of six IBM lines also contrasting in CCS for GH3 and PA2012 experiments (Supplemental Table S2). The IBM lines are from the intermated population of B73xMo17 and were obtained from Shawn Kaeppler, University of Wisconsin, Madison, WI, USA(Senior et al., 1996; Kaeppler et al., 2000)and designated as Mo (Supplemental Table S2). In Malawi, a set of 43 maize landraces was screened for CCS variation in the field (MW2012-1) (Supplemental Table S1). The landrace entries were obtained from Malawi Plant Genetic Resource Center. Based on MW2012-1, a set of six landraces contrasting in CCS was selected for MW2012-2 (Supplemental Table S1).

Greenhouse mesocosm experiments

A total of three experiments were carried out under the same conditions in two consecutive years (Supplemental Table S2). The experiments were conducted in a greenhouse at University Park, PA, USA (40°4'N, 77°49'W), using 14/10 h day/night: 23/20°C day/night: 40-70% relative humidity. The experiments were carried out with natural light between500-1200 µmol photons m^{-2} s^{-1} PAR, and supplemental light between 500-600 µmol photons m^{-2} s^{-1} PAR was provided with 400-W metal-halide bulbs (Energy Technics, York, PA, USA) for 14 h per day. Plants were grown in soil mesocosms consisting of PVC cylinders 1.5 m in height by 0.154 m in diameter, lined with transparent hi-density polyethylene film, which was used to facilitate root sampling. The growth medium consisted of (by volume) 50% commercial grade sand (Quikrete Companies Inc. Harrisburg, PA, USA), 35% vermiculite (Whittemore Companies Inc., Lawrence, MA, USA), 5% Perlite (Whittemore Companies Inc., Harrisburg, PA, USA), and 10% topsoil (Hagerstown silt loam top soil: fine, mixed, mesicTypicHapludalf)). Mineral nutrients were provided by mixing the media with 70g per mesocosm of OSMOCOTE PLUS fertilizer (Scotts-Sierra Horticultural Products Company, Marysville, Ohio, USA)consisting of (in %); N (15), P (9), K (12), S (2.3), B (0.02) Cu (0.05), Fe (0.68), Mn (0.06), Mo (0.02), and Zn (0.05). Seeds were germinated in darkness at 28 ± 1 °C for two d prior to transplanting two seedlings per mesocosm, thinned to one per mesocosm 5 d after planting.

At harvest (i.e. 30 days after planting), the shoot was removed, and the plastic liner was extracted from the mesocosm, cut open and the roots were washed carefully by rinsing the media away with water. This allowed us to recover the entire plant root system. Samples for root respiration measurement were collected 10-20 cm from the base of three representative second whorl crown roots per plant. Root respiration (CO_2 production) was measured 15 - 20 minutes after cutting the

382 shoot using a Li-Cor 6400 (Li-Cor Biosciences, Lincoln, NE, USA) in closed-system mode
383 equipped with a 56 ml chamber. The change in CO_2 concentration in the chamber was monitored
384 for 3 min. During the time of measurement the chamber was placed in a temperature controlled
385 water bath at 27± 1 °C. Following respiration measurements, root segments were preserved in
386 75% ethanol for anatomical analysis as described below.

387 Root length distribution was measured by cutting the root system into 7 segments in 20 cm depth
388 increments. Roots from each increment were spread in a 5 mm layer of water in transparent
389 plexiglass trays and imaged with a flatbed scanner equipped with top lighting (Epson Perfection
390 V700 Photo, Epson America, Inc. USA) at a resolution of 23.6 pixels mm^{-1} (600 dpi). Total root
391 length for each segment was quantified using WinRhizo Pro (Regent Instruments, Québec City,
392 Québec, Canada). Following scanning the roots were dried at $70^{o}C$ for 72 hours and weighed. To
393 summarize the vertical distribution of the root length density we used the D_{95} (Schenk and
394 Jackson, 2002), i.e. the depth above which 95% of the root length.

395 Root segments and leaves were ablated using laser ablation tomography (LAT) (Hall *et al,*
396 unpublished) to obtain images for anatomical analysis. In brief, LAT is a semi-automated system
397 that uses a pulsed laser beam (Avia 7000, 355 nm pulsed laser) to ablate root tissue at the camera
398 focal plane ahead of an imaging stage. The cross-section images were taken using a Canon T3i
399 (Canon Inc. Tokyo, Japan) camera with 5X micro lens (MP-E 65 mm) on the laser-illuminated
400 surface. Root images were analyzed using *RootScan,* an image analysis tool developed for
401 analyzing root anatomy (Burton et al., 2012). CCS was determined from three different images
402 per root segment. CCS was calculated as median cell size. Based on preliminary experiments the
403 cortex was divided into three radial bands: outer (0-0.25 of the cortex from the epidermis), mid-
404 cortical (0.25-0.75) and inner (0.75-1). In this study the median cell size for the mid-cortical band
405 was chosen as a representative value for the root CCS.

406 **Experiment I (GH1)**

407 A randomized complete block design (RCBD) was used in this experiment, with time of planting
408 as a blocking factor replicated three times. A set of 16 IBM lines ((Supplemental Table S2& S3)
409 was planted and water stress was imposed by withholding water starting 14 days after planting.
410 Plants were harvested for root respiration measurements and anatomical analysis 35 days after
411 planting. An experiment was conducted to characterize the pattern cell size variation in different
412 parts of the maize plant. A set of 12 IBM lines was planted in nutrient solution until the two-leaf
413 stage. In this experiment leaf midrib, mesocotyl and primary root each plant were sampled for
414 sectioning. To assess the relationship between cortical cell cross-sectional area and cell length,
415 cortical cell lengths and diameter were measured on laser ablated root longitudinal sections. These
416 measurements were made on mid-cortical region on each of the three sections for each genotype.
417 The cell length or diameter on each section was taken as median of measurements on 20 to 30
418 cells.

419 **Experiment II (GH2) and III (GH3)**

420 Two experiments were conducted, in fall 2011 (GH2) and summer 2012 (GH3). A set of six
421 genotypes was planted in each experiment (Supplemental Table S2& S2). A randomized complete
422 block design (RCBD) with four replications was used in both experiments with time of planting
423 as a blocking factor. Planting was staggered by 7 days. In both experiments, the irrigated

mesocosms (control) each received 200 ml of water every other day, to replenish water lost by evapotranspiration, and in stressed mesocosms, water application was withheld starting 5 days after planting to allow the plants to exploit residual moisture to simulate terminal drought. An SC-1 leaf porometer (Decagon, Pullman, WA) was used for stomatal conductance measurements from the abaxial sides of third fully expanded leaves at 28 days after planting in GH3. All of the stomatal conductance measurements were made between 0900 h and 1100 h. Plants were harvested 30 days after planting for root respiration measurements, root length distribution and shoot biomass. The dry matter of the shoot and root were measured after drying at 70°C for 72 h and root length distribution was determined as described above.

Field experiments Rock Springs, PA, USA

Field sites and experimental setup

Two experiments were conducted in rainout shelters located at the Russell E. Larson Agricultural Research Center in Rock Springs, PA, USA (77°57′W, 40°42′N,), during the summers of 2011 (PA2011) and 2012 (PA2012). The soil is a Hagerstown silt loam (fine, mixed, mesicTypicHapludalf). Both experiments were arranged as split-plots in a randomized complete block design with four replications. The main plots were composed of two moisture regimes and the subplots contained six lines contrasting in cortical cell size. The experiments were hand-planted on 15th June 2011 and 25th June 2012.Both trials were planted in three row plots with 0.75 m inter-row spacing and 0.25 m in-row spacing to give a plant population of 53000 plants ha^{-1}. The drought treatment was initiated 35-40 days after planting using two automated rainout shelters. The shelters (10 by 30 m) were covered with a clear greenhouse plastic film (0.184 mm) and were automatically triggered by rainfall to cover the plots, and excluding natural precipitation throughout the entire growing season. The shelters automatically opened after rainfall, exposing experimental plots to natural ambient conditions whenever it was not raining. Adjacent non-sheltered control plots were rainfed and drip-irrigated when necessary to maintain the soil moisture close to field capacity throughout the growing season. Soil moisture content at different soil depths (20, 35 and 50 cm) was monitored at regular intervals (Supplemental Figure S5), using a TRIME FM system (IMKO, GmbH, Ettlingen, Germany).

Plant measurements

Leaf relative water content (RWC) was used as a physiological indicator of plant water status. To measure leaf RWC, fresh leaf discs (3 cm in diameter) were collected from the third fully expanded leaf for three representative plants per plot 60 days after planting and weighed immediately to determine fresh weight (FW). The discs were then floated in distilled water for 12 h at 4°C with minimal light. Discs were then blotted dry and again weighed to determine turgid weight (TW). After being dried in an oven at 70^{0}C for 72 h, discs were weighed again for dry weight (DW). Leaf RWC was calculated according to (Barrs and Weatherley, 1962).

Root growth and distribution was evaluated by collecting soil cores 80 days after planting. A soil coring tube (Giddings Machine Co., Windsor, CO, USA) 5.1 cm in diameter and 60 cm long was used for sampling. The core was taken midway between plants within a row. The cores were sectioned into 6 segments of 10 cm depth increments and washed. Subsequently the washed roots were scanned using a flatbed scanner (Epson, Perfection V700 Photo, Epson America, Inc. USA)

465 at a resolution of 23.6 pixel mm^{-1} (600 dpi) and analyzed using image processing software
466 WinRhizo Pro (Regent Instruments, Québec city, Québec, Canada).

467 Shoots and roots were evaluated 75 days after planting. To accomplish this, shoots from three
468 representative plants in each plot were cut at soil level. The collected shoot material was dried at
469 $70^{o}C$ for 72 hours and weighed. Root crowns were excavated by the 'shovelomics' method
470 (Trachsel et al., 2011). Three 8-cm root segments were collected 10-20 cm from the base of a
471 second whorl crown root of each plant, and used to assess cortical cell size. The segments were
472 preserved in 75% ethanol before being processed as described above. At physiological maturity,
473 grain yield was collected from 10 plants per plot.

474 **Field experiments – Bunda, Malawi**

475 **Assessing phenotypic variation of CCS in Malawi germplasm (MW2012-1)**

476 The experiment was conducted at Bunda College research farm, Lilongwe, Malawi ($33^{o}48'E$,
477 $14^{o}10'S$,) in 2012 under optimum conditions (i.e. the plots were rainfed but only rarely were they
478 severely moisture stressed). The soil is a Lilongwe series sandy clay loam (Oxic Rhodustalf).The
479 experiment was arranged as randomized complete block design (RCBD) with three replications.
480 Each plot consisted of a single 6 m long row and 25 cm between plants. Root crowns were
481 excavated by 'shovelomics' (Trachsel et al., 2010). Three 8-cm root segments were collected 10-
482 20 cm from the base of a representative second whorl crown root of each plant, and used to assess
483 CCS. The segments were preserved in 75% ethanol before being processed as described above.

484 **Utility of CCS under water limited condition (MW2012-2)**

485 The field experiment was conducted at Bunda College research farm, Lilongwe, Malawi
486 ($33^{o}48'E$, $14^{o}10'S$,) during summer 2012 (i.e. August to November). The area was selected
487 because it is the main maize production area, accounting for more than 20% of the area planted to
488 maize in Malawi per annum, and regarded as having representative soil types and agronomy for
489 maize growing areas in Malawi A set of 6 maize genotypes contrasting in CCS was planted
490 (Supplemental Table S2&S4). The experiment was arranged as split-plot in a randomized
491 complete block design with four replications. The main plots were composed of two moisture
492 regimes and the subplots contained 6 genotypes contrasting in CCS. The trial was planted in
493 single row plots with 0.75 m inter-row spacing and 0.25 m in-row spacing to give a plant
494 population of 53000 plants ha^{-1}. At planting, both the control and stressed plots received the
495 recommended amounts of irrigation. Drought stress was managed by withholding irrigation
496 starting six weeks after planting, so that moisture stress was severe enough to reduce yield and
497 shoot biomass by 30-70%. Control plots, which received supplementary irrigation, were planted
498 alongside the stressed plots separated by a 5 m wide alley. At each location, the recommended
499 fertilizer rate was applied during planting and by top dressing three weeks after planting. Leaf
500 relative water content was determined 60 days after planting as described above. Shoots and roots
501 were evaluated 75 days after planting. The collected shoot material was dried at $70^{o}C$ for 72 hours
502 and weighed. Root crowns were excavated by 'shovelomics'(Trachsel et al., 2011). Three 8-cm
503 root segments were collected 10-20 cm from the base of a representative second whorl crown root
504 of each plant, and used to assess CCS. The segments were preserved in 75% ethanol before being
505 processed as described above. At physiological maturity, grain yield was collected from each plot.

506 **Soil and plant sampling for $\delta^{18}O$ analysis**

In PA2011, soil samples were collected adjacent to plants in the rainout shelter 65 days after planting using a 5 cm diameter soil core. Soil cores were taken to the maximum achievable depth of 60 cm. The cores were immediately separated into 10 cm increments; 10, 20, 30, 40 50, and 60 cm. The corresponding maize stems were collected at the same time that soil was sampled, approximately 8-10 cm of the stem was collected just aboveground level and the epidermis was immediately removed. Soil and maize stem samples were put in a snap vials, sealed with parafilm to prevent evaporation, and refrigerated immediately. Cryogenic vacuum distillation (West et al., 2006; Koeniger et al., 2010) was used to extract soil water and crop stem water. In cryogenic vacuum distillation, two glass tubes were attached to a vacuum pump. The sample was placed in one tube and frozen by submerging the tube in liquid nitrogen, and then both tubes were evacuated by vacuum pump to create a closed U-shape configuration. After that, the tube containing sample was heated, while the collection tube was still immersed in liquid nitrogen to catch the vapor. Samples were weighed and oven dried after extraction to ensure the extraction time was sufficient to vaporize all the water in samples. The water samples were analyzed at the Penn State Institutes of Energy and the Environment (PSIEE). Stable isotopic analyses were performed using a PICARRO L2130-i δD/δ18O Ultra High Precision Isotopic Water Analyzer (PICARRO Inc, CA, USA). Results were expressed as parts per thousand deviations from the Vienna Standard Mean Ocean Water (VSMOW). To determine the percent contribution of soil water at depth to the signature of water within the plant's xylem, an isotopic mixing model was used (Phillips et al., 2005). IsoSource Version 1.3.1 (Phillips and Gregg, 2003) was used to evaluate the relative contribution of each soil layer to plant xylem water signature. The fractional increment was set at 1%, and tolerance at 0.1.

Data analysis

Data from each year were analyzed separately since different sets of genotypes were used. For mesocosm data, for comparisons of genotypes, irrigation levels and their interaction effects, a two-way ANOVA was used. Field data were analyzed as a randomized complete block split plot design to determine the presence of significant effects due to soil moisture regime, genotype (or phenotype group) and interaction effects on the measured and calculated parameters. Mean separation of genotypes for the different parameters was performed by a Tukey-HSD test. Unless otherwise noted, $HSD_{0.05}$ values were only reported when the F-test was significant at $P \leq 0.05$. Linear regression analysis was used to establish relationships between CCS and measured or calculated parameters. Data was analyzed using R version 3.0.0(R Development Core Team, 2014).

LITERATURE CITED

Araus JL, Slafer G a., Royo C, Serret MD (2008) Breeding for Yield Potential and Stress Adaptation in Cereals. CRC Crit Rev Plant Sci **27**: 377–412

Barrs HD, Weatherley PE (1962) A re-examination of the relative turgidity technique for estimating water deficits in leaves. Aust J Biol Sci **15**: 413–428

Boyer JS, Westgate ME (2004) Grain yields with limited water. J Exp Bot **55**: 2385–2394

Burke MB, Lobell DB, Guarino L (2009) Shifts in African crop climates by 2050, and the implications for crop improvement and genetic resources conservation. Glob Environ Chang **19**: 317–325

Burton AL, Brown KM, Lynch JP (2013) Phenotypic diversity of root anatomical and architectural traits in Zea species. Crop Sci **53**: 1042–1055

Burton AL, Williams MS, Lynch JP, Brown KM (2012) RootScan: Software for high-throughput analysis of root anatomical traits. Plant Soil **357**: 189–203

Chevalier C, Bourdon M, Pirrello J, Cheniclet C, Gévaudant F, Frangne N (2013) Endoreduplication and fruit growth in tomato: evidence in favour of the karyoplasmic ratio theory. J Exp Bot. doi: 10.1093/jxb/ert366

Chimungu JG, Brown KM, Lynch JP (2014) Reduced root cortical cell file number improves drought tolerance in maize. Plant Physiol. provisiona:

Cox WJ, Cherney JH (2012) Lack of Hybrid, Seeding, and Nitrogen Rate Interactions for Corn Growth and Yield. Agron J **104**: 945–952

Dawson TE, Pate JS (1996) Seasonal water uptake and movement in root systems of Australian phraeatophytic plants of dimorphic root morphology: a stable isotope investigation. Oecologia **107**: 13–20

Dornhoff G, Shibles R (1976) Leaf morphology and anatomy in relation to CO2-exchange rate of soybean leaves. Crop Sci **16**: 377–381

Edmeades GO (2008) Drought tolerance in maize: an emerging reality. . A Featur. James, Clive. 2008. Glob. Status Commer. Biotech/GM Crop. 2008. ISAAA Br. No. 39. ISAAA Ithaca, NY

Edmeades GO (2013) Progress in achieving and delivering drought tolerance in maize - An update. An Updat. ISAAA Ithaca, NY.

Ehleringer JR, Dawson TE (1992) Water uptake by plants: perspectives from stable isotope composition. Plant Cell Environ **15**: 1073–1082

Ehleringer JR, Roden J, Dawson TE (2000) Assessing ecosystem-level water relations through stable isotopes ratio analyses. *In* OE Sala, RB Jackson, HA Mooney, RW Howarth, eds, Methods Ecosyst. Sci. Springer-Verlag, pp 181–198

El-Sharkawy M, Hesketh J (1965) Photosynthesis among species in relation to characteristics of leaf anatomy and CO2 diffusion resistances. Crop Sci **4**: 517–521

El-sharkawy MA (2009) Pioneering research on C4 photosynthesis : Implications for crop water relations and productivity in comparison to C3 cropping systems. J Food, Agric Environ **7**: 468–484

579 **Evans DE** (2004) Aerenchyma formation. New Phytol **161**: 35–49

580 **Fan M, Zhu J, Richards C, Brown KM, Lynch JP** (2003) Physiological roles for aerenchyma
581 in phosphorus-stressed roots. Funct Plant Biol **30**: 493–506

582 **IPCC** (2014) Climate change 2014: Impacts, adaptation, and vulnerability. Working Group II
583 Contribution to the IPCC 5th Assessment Report.

584 **Jaramillo RE, Nord EA, Chimungu JG, Brown KM, Lynch JP** (2013) Root cortical burden
585 influences drought tolerance in maize. Ann Bot **112**: 1–9

586 **Kaeppler SM, Parke JL, Mueller SM, Senior L, Stuber C, Tracy WF** (2000) Variation among
587 maize inbred lines and detection of quantitative trait loci for growth at low phosphorus and
588 responsiveness to arbuscular mycorrhizal fungi. Crop Sci **40**: 358–364

589 **Koeniger P, Leibundgut C, Link T, Marshall JD** (2010) Stable isotopes applied as water
590 tracers in column and field studies. Org Geochem **41**: 31–40

591 **Lambers H, Atkin OK, Millenaar FF** (2002) Respiratory patterns in roots in relation to their
592 functioning. *In* Y Waisel, A Eshel, K Kafkaki, eds, Plant Roots, Hidden Half, Third Edit. Marcel
593 Dekker, Inc, New York, New York, pp 521–552

594 **Lobell DB, Bänziger M, Magorokosho C, Vivek B** (2011a) Nonlinear heat effects on African
595 maize as evidenced by historical yield trials. Nat Clim Chang **1**: 42–45

596 **Lobell DB, Schlenker W, Costa-Roberts J** (2011b) Climate trends and global crop production
597 since 1980. Science **333**: 616–20

598 **Lynch J** (2014) Root phenes that reduce the metabolic costs of soil exploration: opportunities for
599 21st century agriculture. Plant. Cell Environ. in press:

600 **Lynch JP** (2007) Roots of the second green revolution. Aust J Bot **55**: 493–512

601 **Lynch JP** (2011) Root phenes for enhanced soil exploration and phosphorus acquisition: tools for
602 future crops. Plant Physiol **156**: 1041–1049

603 **Lynch JP** (2013) Steep, cheap and deep: an ideotype to optimize water and N acquisition by
604 maize root systems. Ann Bot **112**: 347–357

605 **Lynch JP, Chimungu JG, Brown KM** (2014) Root anatomical phenes associated with water
606 acquisition from drying soil: targets for crop improvement. J. Exp. Bot. in press:

607 **Lynch JP, Ho MD** (2005) Rhizoeconomics: Carbon costs of phosphorus acquisition. Plant Soil
608 **269**: 45–56

Marshall WF, Young KD, Swaffer M, Wood E, Nurse P, Kimura A, Frankel J, Wallingford J, Walbot V, Qu X, et al (2012) What determines cell size? BMC Biol **10:101**: 1–22

Miller CR, Ochoa I, Nielsen KL, Beck D, Lynch JP (2003) Genetic variation for adventitious rooting in response to low phosphorus availability: potential utility for phosphorus acquisition from stratified soils. Funct Plant Biol **30**: 973–985

Nielsen KL, Eshel A, Lynch JP (2001) The effect of phosphorus availability on the carbon economy of contrasting common bean (*Phaseolus vulgaris* L.) genotypes. J Exp Bot **52**: 329–339

Nielsen RL (2012) Thoughts on seeding rates for corn. Purdue Corny News Netw. Artic. Purdue Univ. Dep. Agron.,

Palta J, Gregory P (1997) Drought affects the fluxes of carbon to roots and soil in 13 C pulse-labelled plants of wheat. Soil Biol Biochem **29**: 1395–1403

Phillips DL, Gregg JW (2003) Source partitioning using stable isotopes: coping with too many sources. Oecologia **136**: 261–269

Phillips DL, Newsome SD, Gregg JW (2005) Combining sources in stable isotope mixing models: alternative methods. Oecologia **144**: 520–527

Postma JA, Lynch JP (2011a) Theoretical evidence for the functional benefit of root cortical aerenchyma in soils with low phosphorus availability. Ann Bot **107**: 829–841

Postma JA, Lynch JP (2011b) Root cortical aerenchyma enhances the growth of maize on soils with suboptimal availability of nitrogen, phosphorus, and potassium. Plant Physiol **156**: 1190–1201

R Development Core Team R (2014) R: A language and environment for statistical computing. R Foundation for Statistical Computing. R Found. Stat. Comput.,

Reeves GW, Cox WJ (2013) Inconsistent Responses of Corn to Seeding Rates in Field-Scale Studies. Agron J **105**: 693–704

Richards RA, Rebetzke GJ, Watt M, Condon AG, Spielmeyer W, Dolferus R (2010) Breeding for improved water productivity in temperate cereals: phenotyping, quantitative trait loci, markers and the selection environment. Funct Plant Biol **37**: 85–97

Richardson AE, Lynch JP, Ryan PR, Delhaize E, Smith FA, Smith SE, Harvey PR, Ryan MH, Veneklaas EJ, Lambers H, et al (2011) Plant and microbial strategies to improve the phosphorus efficiency of agriculture. Plant Soil **349**: 121–156

Sablowski R, Carnier Dornelas M (2013) Interplay between cell growth and cell cycle in plants. J Exp Bot. doi: 10.1093/jxb/ert354

641 **Saengwilai P, Nord EA, Brown KM, Lynch JP** (2014a) Root cortical aerenchyma enhances
642 nitrogen acquisition from low nitrogen soils in maize (Zea mays L.). Plant Physiol. June 2014
643 pp.114.241711

644 **Saengwilai P, Tian X, Lynch J** (2014b) Low crown root number enhances nitrogen acquisition
645 from low nitrogen soils in maize (*Zea mays* L.). Plant Physiol. doi: 10.1104/pp.113.232603

646 **Schenk HJ, Jackson RB** (2002) The Global Biogeography of Roots. Ecol Monogr **72**: 311–328

647 **Schlenker W, Lobell DB** (2010) Robust negative impacts of climate change on African
648 agriculture. Environ Res Lett. doi: 10.1088/1748-9326/5/1/014010

649 **Senior ML, Chin ECL, Lee M, Smith JSC, Stuber CW** (1996) Simple sequence repeat markers
650 developed from maize sequences found in Genbank database: Map construction. Crop Sci **36**:
651 1676–1683

652 **Sharp R, Davies W** (1979) Solute regulation and growth by roots and shoots of water-stressed
653 maize plants. Planta **4349**: 43–49

654 **Smucker AJM** (1993) Soil environmental modifications of root dynamics and measurement.
655 Annu Rev Phytopathol **31**: 191–216

656 **St.Clair SB, Lynch JP** (2010) The opening of Pandora's box: climate change impacts on soil
657 fertility and crop nutrition in developing countries. Plant Soil DOI 10.100:

658 **Striker GG, Insausti P, Grimoldi a. a., Vega a. S** (2007) Trade-off between root porosity and
659 mechanical strength in species with different types of aerenchyma. Plant Cell Environ **30**: 580–
660 589

661 **Sugimoto-Shirasu K, Roberts K** (2003) "Big it up": endoreduplication and cell-size control in
662 plants. Curr Opin Plant Biol **6**: 544–553

663 **Taiz L** (1992) The plant vacuole. J Exp Biol **172**: 113–122

664 **Trachsel S, Kaeppler SM, Brown KM, Lynch JP** (2011) Shovelomics : high throughput
665 phenotyping of maize (*Zea mays* L .) root architecture in the field. Plant Soil **314**: 75–87

666 **Tuberosa R, Salvi S** (2006) Genomics-based approaches to improve drought tolerance of crops.
667 Trends Plant Sci **11**: 405

668 **Warner D a, Edwards GE** (1989) Effects of polyploidy on photosynthetic rates, photosynthetic
669 enzymes, contents of DNA, chlorophyll, and sizes and numbers of photosynthetic cells in the C(4)
670 dicot atriplex confertifolia. Plant Physiol **91**: 1143–1151

671 **Warner DA, Edwards GE** (1988) C 4 photosynthesis and leaf anatomy in diploid and
672 autotetraploid *Pennisetum americanum*(pearl millet). Plant Sci **56**: 85–92

673 **Warner DA, Ku MSB, Edwards GE** (1987) Photosynthesis, leaf anatomy, and cellular
674 constituents in the polyploid C4 grass *Panicum virgatum*. Plant Physiol **84**: 461–466

675 **Wasson P, Richards R, Chatrath R, Misra SC, Prasad SVS, Rebetzke GJ, Kirkegaard JA,**
676 **Christopher J, Watt M** (2012) Traits and selection strategies to improve root systems and water
677 uptake in water-limited wheat crops. J Exp Bot **63**: 3485–3498

678 **Weijschedé J, Antonise K, de Caluwe H, de Kroon H, Huber H** (2008) Effects of cell number
679 and cell size on petiole length variation in a stoloniferous herb. Am J Bot **95**: 41–49

680 **West AG, Patrickson SJ, Ehleringer JR** (2006) Water extraction times for plant and soil
681 materials used in stable isotope analysis. Rapid Commun Mass Spectrom Mass **20**: 1317–1321

682 **Wilson D, Cooper J** (1970) Effect of selection for mesophyll cell size on growth and assimilation
683 in *Lolium perenne* L. New Phytol **69**: 233–245

684 **York LM, Nord E a., Lynch JP** (2013) Integration of root phenes for soil resource acquisition.
685 Front Plant Sci **4**: 1–15

686 **Zhu J, Brown KM, Lynch JP** (2010) Root cortical aerenchyma improves the drought tolerance
687 of maize (*Zea mays* L.). Plant Cell Environ **33**: 740–749

688

689

690 **Figure Legends**

691 **Figure 1.** Cross-sectional images of second nodal crown roots of maize showing genotypic
692 difference in root cortical cell size. The roots were ablated 10 to 20 cm from the base. The black
693 scale bar at bottom left represents 100 microns in length. The images were obtained using laser
694 ablation tomography.

695 **Figure 2.**The relationship between root respiration per unit length and cortical cell size for GH1
696 (r^2=0.46, p=0.009), GH2 (r^2=0.59, p=0.001) and in GH3 (r^2=0.52, p=0.018) in greenhouse
697 mesocosms30 days after planting. Each point is the mean of at least three measurements of
698 respiration.

699 **Figure 3.**The relationship between root depth (D_{95}) and cortical cell size for GH2(r^2 = 0.48, p =
700 0.001) and GH3 (r^2 = 0.45, p = 0.01) in the greenhouse mesocosms 30 days after planting. The
701 regression line is only shown for the significant relationships. Data include both water stressed
702 (WS) and well watered (WW) conditions. D_{95} measures the depth above which 95% of root
703 length is present in mesocosms.

704 **Figure 4.** Carbon dioxide exchange rate (A) and stomatal conductance (B) for genotypes with
705 large and small cortical cells in the greenhouse mesocosms (GH3) 30 days after planting both
706 under water stressed (WS) and well watered (WW) conditions. Data shown are means ± SE of the
707 means for three lines per group (n = 4). Means with the same letters are not significantly different
708 (p< 0.05).

709 **Figure 5.** The relationship between root depth (D_{95}) and cortical cell size for PA2011(r^2 = 0.41, p
710 = 0.01) and PA2012(r^2 = 0.42, p = 0.05) in the field 80 days after planting both under water
711 stressed (WS) and well watered (WW) conditions. The regression line is only shown for the
712 significant relationship. D_{95} is the depth above where 95 % of the root length is present in the soil
713 profile.

714 **Figure 6.** Leaf relative water content for genotypes with large and small cortical cells at 60 days
715 after planting (DAP) in the field **(A)** PA2011, **(B)** PA2012 and **(C)** MW2012-2 both in well-
716 watered **(WW)** and water-stressed **(WS)** conditions. Data shown are means ± SE of the means for
717 three lines per group (n = 4). Means with the same letters are not significantly different (p< 0.05).

718 **Figure 7**. Soil water oxygen isotope composition ± S.E. in six soil layers in the rainout shelters
719 (PA2011). Sampling was done 65 days after planting. Values are the means ±SE of 3 observation
720 points in the rainout shelters.

721 **Figure 8.** Shoot biomass for genotypes with large and small cortical cells in the mesocosms 30
722 days after planting **(A)**GH2 and **(B)**GH3 in the mesocosms both in well-watered **(WW)** and
723 water-stressed **(WS)** conditions. Data shown are means ± SE of the means for three lines per
724 group (n = 4). Means with the same letters are not significantly different (p< 0.05).

Figure 9. Shoot biomass for genotypes with large and small cortical cells in the field 70 days after planting **(A)** PA2011, **(B)** 2012, and **(C)** MW2012-2 both water-stressed (WS) and well-watered (WW) conditions. Data shown are means ± SE of the means for three lines per group (n = 4). Means with the same letters are not significantly different ($p < 0.05$).

Figure 10. Grain yield for genotypes with large and small cortical cells in the field **(A)** PA2012 and **(B)** MW2012-2 both water-stressed (WS) and well-watered (WW) conditions. Data shown are means ± SE of the means (n = 4). Means with the same letters are not significantly different ($p < 0.05$).

Supplemental Figures

Supplemental Figure S1. Transverse section showing parenchyma cells in maize for (A) leaf midrib, (B) mesocotyl cortex and (C) root cortex for the same plant. The black scale bar in bottom left represents 100 microns in length. The images were obtained using laser ablation tomography.

Supplemental Figure S2. Correlation between cortical cell diameter and cell length ($y = 1.802x + 24.^2 = 0.2309$).

Supplemental Figure S3. Root length density at different soil depths for genotypes with large CCS and small CCS under water stressed (WS) and well watered (WW) conditions in the greenhouse (GH1) with corresponding D_{95}. D_{95} measures the depth above where 95% of root length is present.

Supplemental Figure S4. Root length density at different soil depths for genotypes with large CCS and small CCS under water stressed (WS) and well watered (WW) conditions in the field (PA2011) with corresponding D_{95}. D_{95} measures the depth above where 95% of root length is present.

Supplemental Figure S5. Change in soil moisture content at different depths (15cm, 30cm, and 50cm) in well watered (WW) and water stressed (WS) plots for PA2012. Terminal drought was imposed in WS plots beginning at 30 DAP.

Tables

Table 1. Summary of analysis of variance (F- ratio) for the effects of soil moisture regime (treatment) and genotype on shoot biomass, rooting depth (D_{95}), and stomatal conductance in greenhouse mesocosm experiments (GH2 and GH3).

	GH2		GH3		
Effect	Biomass	D_{95}	Biomass	D_{95}	Conductance
Treatment (T)	51.04**	46.89**	32.47**	29.80**	16.02**
Genotype (G)	9.77**	6.91**	15.39**	15.29*	5.09*
G*T	2.70¶	6.75**	28.86**	11.86*	0.72

p from 0.1 to 0.05; **p* from 0.05 to 0.01; ***p* from 0.01 to 0.001. D_{95} is the depth above which 95% of root length is found in mesocosms, Treatment is the moisture regimes imposed; Genotype is phenotype class (i.e. large CCS and small CCS); and Conductance is the stomatal conductance (mol $m^{-2}s^{-1}$).

759

760 **Table 2.** Summary of analysis of variance (F-ratio) for the effects of soil moisture regime (treatment) and genotype on yield, shoot
761 biomass, rooting depth (D_{95}), and leaf relative water content (RWC) in three field experiments (PA2011, PA2012 and MW2012-2).

	PA2011			PA2012				MW2012-2		
Effect	Biomass	D_{95}	RWC	Biomass	D_{95}	RWC	Yield	Biomass	RWC	Yield
Treatment (T)	49.5***	6.5*	21.0***	41.3***	4.9*	35.7***	46.2***	166.0***	58.8***	81.49***
Genotype (G)	6.7**	7.2***	9.7***	3.9**	0.6ns	9.8**	10.1***	23.6***	2.0*	20.0**
G x T	4.3**	1.6*	5.7**	5.5***	0.3ns	4.2**	10.7***	13.4***	8.0***	16.6***

762 *p from 0.05 to 0.01: **p from 0.01 to 0.001: ***p< 0.001. D_{95} is the depth above which 95% of root length is found in soil profile, Treatment is the moisture
763 regimes imposed; Genotype is the phenotype class (large CCS and small CCS); RWC is the leaf relative water content (%).

Table 3. Means of $\delta^{18}O$ of xylem water ± SE measured for six genotypes contrasting in CCS under water stress 65 days after planting. Proportional water use by depth from different soil layers where "deep" is the aggregate of three deep soil layers (Fig 7) calculated using multi-source mixing model analysis (Phillips et al., 2005).

Classification based on CCS	RIL	$\delta^{18}O$ of xylem water	Proportional water use by depth (%)		
			10 cm	20 cm	Deep
Large CCS	26	-7.9±0.306	0	35	65
	59	-8.0±0.105	0	24	76
	178	-8.9±0.19	0	2	98
Small CCS	131	-6.4±0.253	0	81	19
	132	-6.2±0.166	0	93	7

Supplemental Tables

Supplemental Table S1. Descriptive statistics of root cortical cell size variation (cross sectional area in um^2) for maize in the greenhouse (GH1) and in the field (MW2012-1). The cortex was divided into three bands: the outer band (outer 25% of the cortex), mid-cortical band (middle 50% of the cortex) and inner band (inner 25% of the cortex).

Experiment	Variable	Minimum	Maximum	Coefficient of Variation (%)
MW2012-1	Outer band (0-0.25)	79.4	175.4	20.2
	Mid-cortical band (0.25-0.75)	101.5	514.6	37.6
	Inner band (0.75-1)	80.5	196.0	24.4
GH1	Outer band (0-0.25)	81.4	187.7	25.4
	Mid-cortical band (0.25-0.75)	151.4	533.9	38.4
	Inner band (0.75-1)	74.5	158.5	17.4

785

786

787

788

789

790

791

792

793

794 **Supplemental Table S2.**Summary of the experiments. The small CCS selection group had cell
795 sizes from 127 to 217 (mean = 166 ± 5) and large CCS selection group from 239 to 551 (mean =
796 411 ± 16). Rep is the number of replicates in each experiment.

Experiment	[a]ID	Environment	Rep	Group by phenotype	RILs
Experiment 1	GH1	Greenhouse	3	NA	Mo, 026, 059, 090, 126, 131, 132, 201, 224, 233, 277, 284,323,344,345, 317, 365
Experiment 2	GH2	Greenhouse	4	Large CCS Small CCS	Mo178, 059,026 Mo284, 181
Experiment 3	GH3	Greenhouse	4	Large CCS Small CCS	Mo201,090,126 Mo039,323,344
Experiment 4	PA2011	Field-PA, USA	4	Large CCS Small CCS	Mo178, 059,026 Mo131, 132
Experiment 5	PA2012	Field-PA, USA	4	Large CCS Small CCS	Mo201,090,126 Mo039,323,344
Experiment 6	MW2012-1	Field-Bunda, MW		NA	MW139, 145, 148, 163, 164, 172, 193, 203, 218, 243, 249, 250, 260, 297, 303, 386, 403, 539, 569, 629, 637, 696, 699, 699, 736, 741, 750, 752, 787, 811, 1772, 1786, 1857, 1915, 1992, 2012, 2027, 2862, 3243, 3244, 3411, Mkangala, SW19
Experiment 7	MW2012-2	Field-Bunda, MW	4	Large CCS Small CCS	MW297,386,696 MW1772,218,629

797 [a]ID based on year and where the experiment was conducted

Supplemental Table S3. List of genotypes selected from IBM population and root anatomical phenes; RD, root diameter, TCA, total cortical area, SD, stele diameter, root cortical aerenchyma (RCA), and CCFN, cortical cell file number. The data shown are means of 4 replicates ± SE of the mean

Treatment	RIL	Group by phenotype	RD (mm)	TCA (mm2)	Stele Diameter (mm)	%RCA	CCFN
WS	Mo026	Large CCS	0.9±0.1	0.5±0.1	0.4±0.1	0.1±0.1	9.3±0.5
WW	Mo026	Large CCS	1.3±0.2	1±0.3	0.5±0.1	0.1±0.1	10.3±1.1
WW	Mo059	Large CCS	1.5±0.1	1.4±0.1	0.7±0.2	0.2±0.2	12.1±0.8
WS	Mo059	Large CCS	1.3±0.2	1.0±0.1	0.6±0.1	0.2±0.1	10.2±0.7
WS	Mo090	Large CCS	1.8±0.2	2.1±0.3	0.6±0.1	0±0	10.4±0.4
WW	Mo090	Large CCS	1.7±0.2	1.9±0.3	0.6±0.1	0±0	11.8±1.1
WW	Mo126	Large CCS	1.5±0.2	1.5±0.3	0.6±0.2	0.2±0.2	12.1±0.9
WS	Mo126	Large CCS	1.5±0.1	1.3±0.2	0.7±0.1	0.1±0.1	12.3±1.0
WS	Mo178	Large CCS	1.2±0.1	1±0.1	0.6±0.1	0±0	8.6±0.5
WW	Mo178	Large CCS	1.4±0.1	1.2±0.1	0.7±0.1	0.1±0.1	8.6±0.3
WS	Mo201	Large CCS	1.3±0.1	1.1±0.1	0.5±0.1	0±0	8±0
WW	Mo201	Large CCS	1.7±0.1	1.8±0.2	0.7±0.1	0.1±0.1	10.5±0.6
WS	Mo131	Small CCS	1.3±0.1	0.9±0.1	0.6±0.1	0.3±0.1	9.8±0.5
WW	Mo131	Small CCS	1.4±0.2	1.2±0.2	0.6±0.1	0.3±0.1	10.3±0.5
WS	Mo132	Small CCS	1±0.1	0.6±0.1	0.5±0.1	0.1±0.1	8.5±0.3
WW	Mo132	Small CCS	1.5±0.2	1.3±0.3	0.7±0.1	0.2±0.1	8.3±0.3
WS	Mo181	Small CCS	1±0.1	0.6±0.1	0.5±0.1	0.1±0.1	12.0±0.8
WW	Mo181	Small CCS	1.2±0.1	0.9±0.1	0.5±0.1	0.3±0.1	13.0±0
WS	Mo284	Small CCS	1.2±0.1	0.9±0.1	0.5±0.1	0.3±0.1	12.8±0.3
WW	Mo284	Small CCS	1.3±0.2	1.1±0.4	0.6±0.1	0.3±0.1	12.0±0.8
WS	Mo039	Small CCS	1.6±0.3	1.7±0.4	0.7±0.2	0±0	11.2±2.1
WW	Mo039	Small CCS	1.4±0.1	1.2±0.2	0.6±0.1	0.1±0.1	11.5±1.2
WS	Mo323	Small CCS	1.3±0.1	1.1±0.1	0.6±0.1	0.1±0.1	8.8±0.3
WW	Mo323	Small CCS	1.7±0.1	1.8±0.3	0.7±0.1	0.1±0.1	10.5±0.8
WS	Mo344	Small CCS	1.3±0.1	1±0.1	0.6±0.1	0±0	9.6±0.5
WW	Mo344	Small CCS	1.5±0.1	1.4±0.2	0.7±0.1	0±0	11.5±0.9

811

812

813

814

815

816

817

818

819 **Supplemental Table S4.**List of genotypes selected from Malawi maize breeding program
820 populations and root anatomical phenes; RD, root diameter, TCA, total cortical area, SD, stele
821 diameter, root cortical aerenchyma (RCA), and CCFN, cortical cell file number. The data shown
822 are means of 4 replicates ± SE of the mean

Soil moisture regimes	RIL	Group by phenotype	RD (mm)	TCA (mm^2)	Stele Diameter (mm)	%RCA	CCFN
WS	218	Small CCS	1.5±0.1	1.5±0.2	0.8±0.1	0.1±0.1	12.4±1.5
WW	218	Small CCS	1.6±0.1	1.5±0.2	0.8±0.1	0.1±0.1	13.2±0.5
WS	629	Small CCS	1.7±0.1	1.8±0.1	0.9±0.1	0.1±0.1	15.5±0.7
WW	629	Small CCS	1.7±0.1	1.7±0.1	0.8±0.1	0.1±0.1	12.2±1
WS	1772	Small CCS	1.6±0.1	1.7±0.2	0.8±0.1	0±0	12.1±0.7
WW	1772	Small CCS	1.4±0.1	1.3±0.2	0.7±0.1	0.1±0.1	9.2±0.4
WS	297	Large CCS	1.7±0.1	1.5±0.1	0.9±0.1	0.1±0.1	12.6±1.1
WW	297	Large CCS	1.7±0.1	1.7±0.1	0.8±0.1	0.2±0.1	12.8±0.8
WS	386	Large CCS	1.6±0.1	1.5±0.2	0.8±0.1	0.1±0.1	10.7±0.5
WW	386	Large CCS	1.6±0.1	1.5±0.1	0.8±0.1	0.1±0.1	12±0.9
WS	696	Large CCS	1.6±0.1	1.6±0.2	0.7±0.1	0.1±0.1	12.3±0.6
WW	696	Large CCS	1.7±0.1	1.7±0.2	0.8±0.1	0.2±0.1	13.7±1

823

824

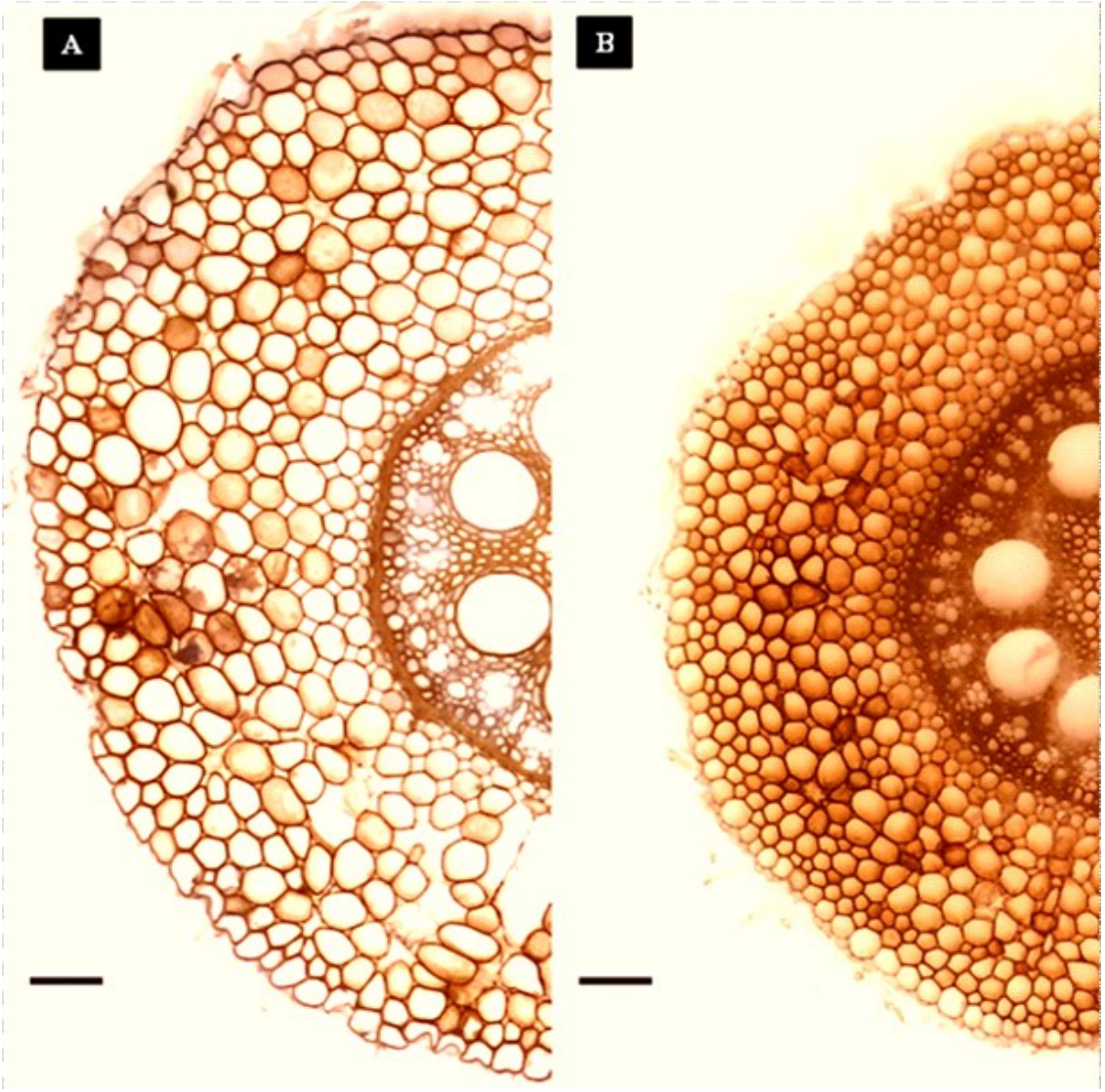

Figure 1. Cross-sectional images of second nodal crown roots of maize showing genotypic difference in root cortical cell size. The roots were ablated 10 to 20 cm from the base. The black scale bar at bottom left represents 100 microns in length. The images were obtained using laser ablation tomography.

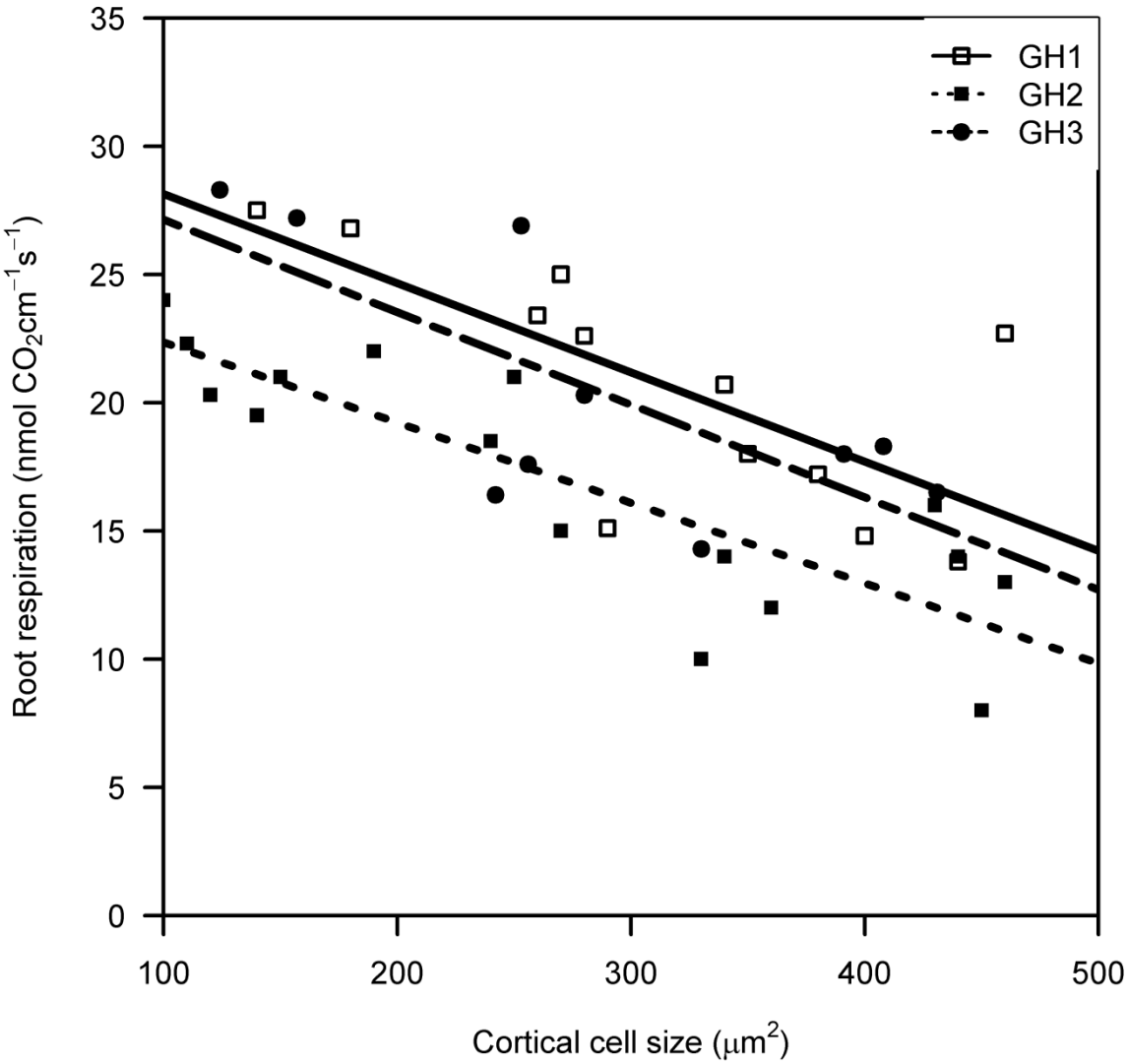

Figure 2. The relationship between root respiration per unit length and cortical cell size for GH1 (r^2=0.46, *p*=0.009), GH2 (r^2=0.59, *p*=0.001) and in GH3 (r^2=0.52, *p*=0.018) in greenhouse mesocosms30 days after planting. Each point is the mean of at least three measurements of respiration.

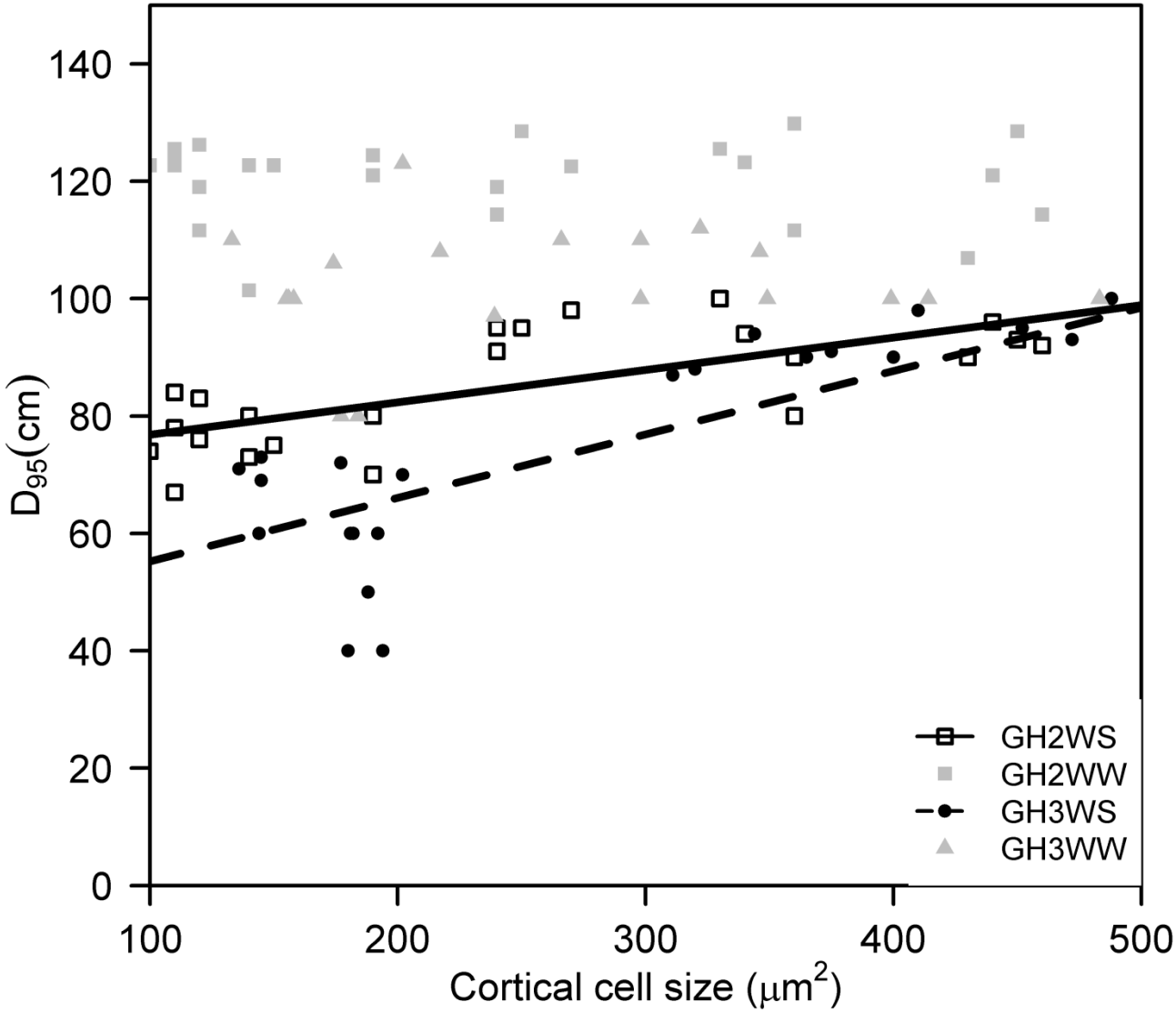

Figure 3. The relationship between root depth (D_{95}) and cortical cell size for GH2(r^2 = 0.48, p = 0.001) and GH3 (r^2 = 0.45, p = 0.01) in the greenhouse mesocosms 30 days after planting. The regression line is only shown for the significant relationships. Data include both water stressed (WS) and well watered (WW) conditions. D_{95} measures the depth above which 95% of root length is present in mesocosms.

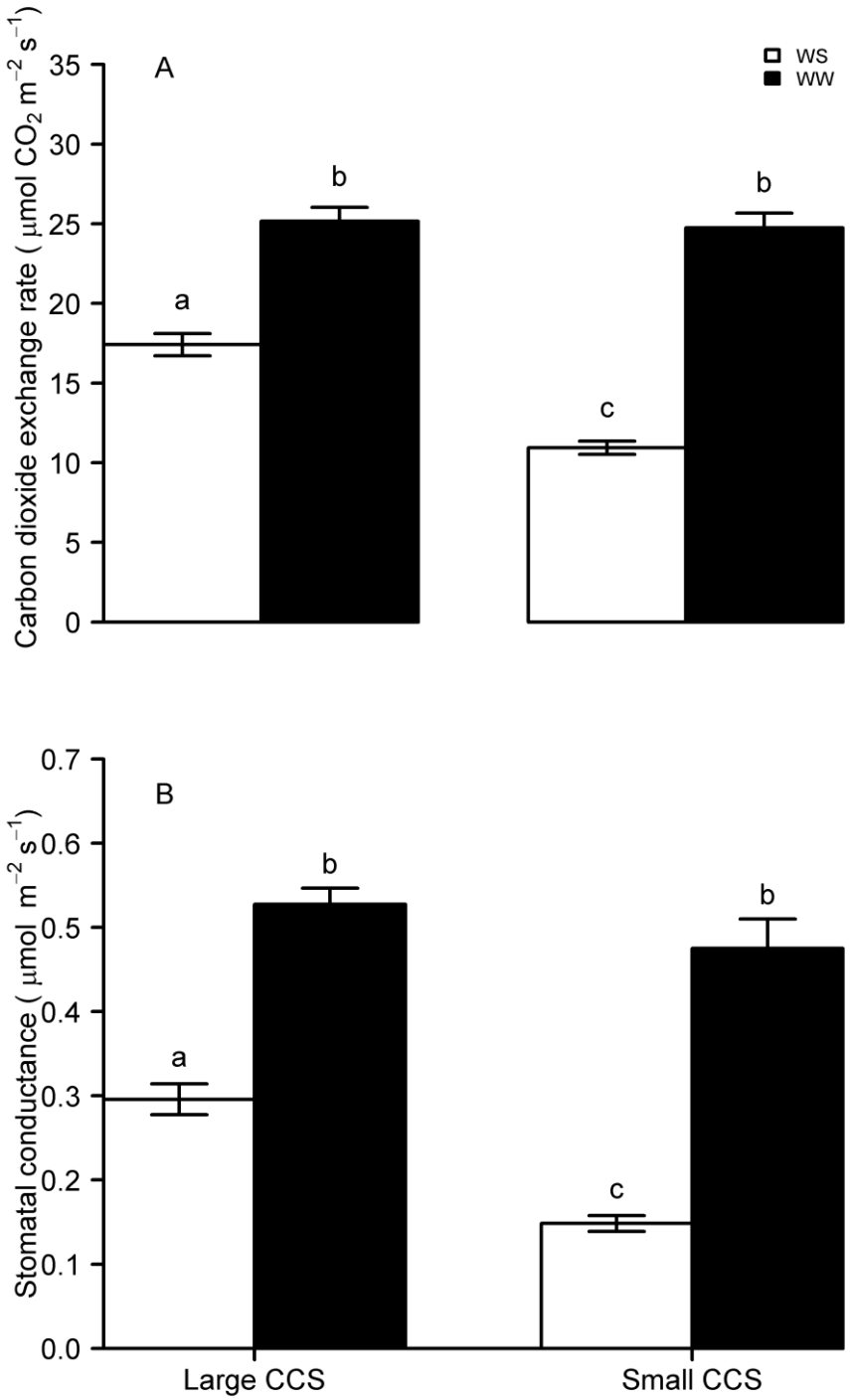

Figure 4. Carbon dioxide exchange rate (A) and stomatal conductance (B) for genotypes with large and small cortical cells in the greenhouse mesocosms (GH3) 30 days after planting both under water stressed (WS) and well watered (WW) conditions. Data shown are means ± SE of the means for three lines per group (n = 4). Means with the same letters are not significantly different ($p < 0.05$).

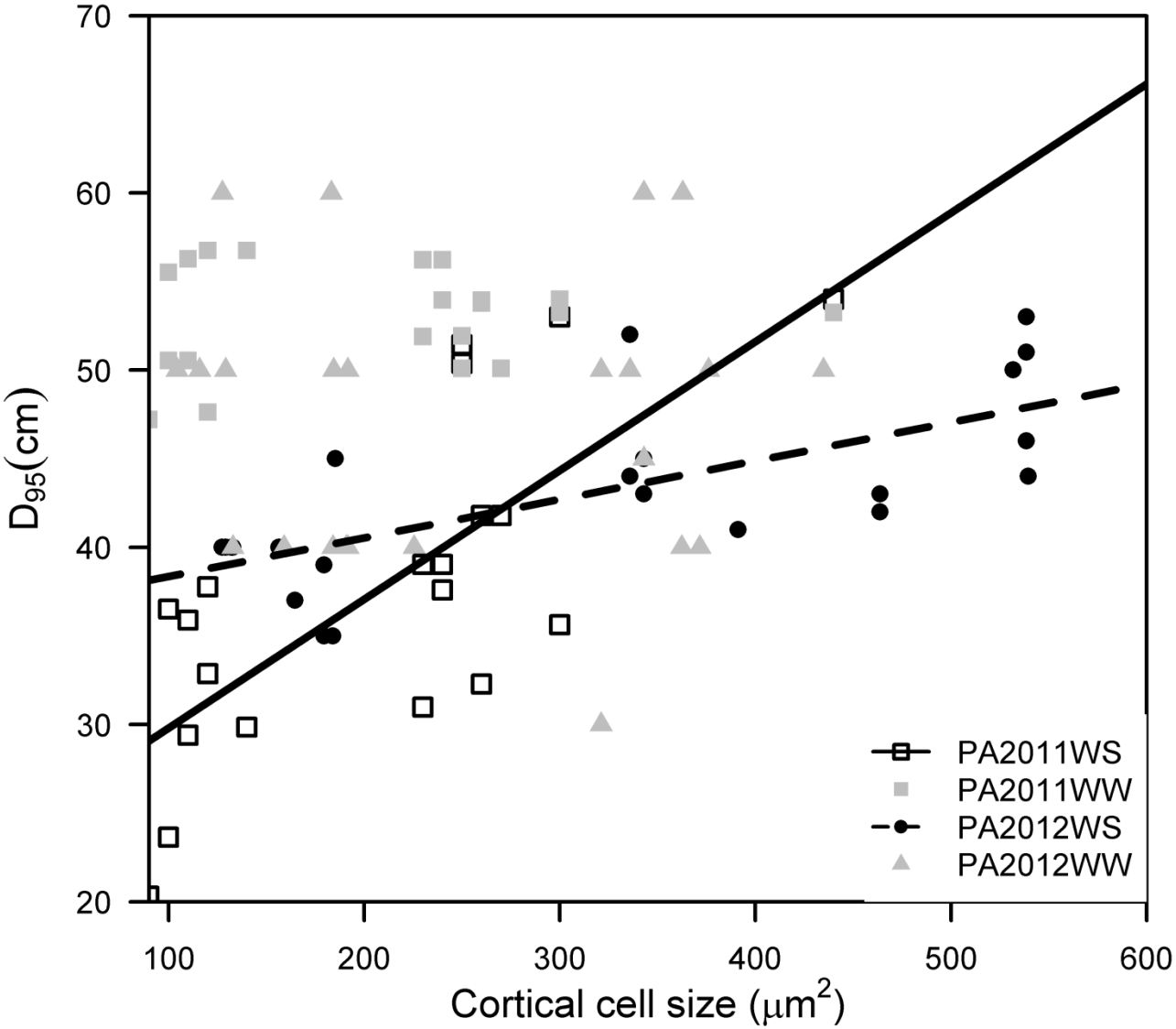

Figure 5. The relationship between root depth (D_{95}) and cortical cell size for PA2011(r^2 = 0.41, *p* = 0.01) and PA2012(r^2 = 0.42, *p* = 0.05) in the field 80 days after planting both under water stressed (WS) and well watered (WW) conditions. The regression line is only shown for the significant relationship. D_{95} is the depth above where 95 % of the root length is present in the soil profile.

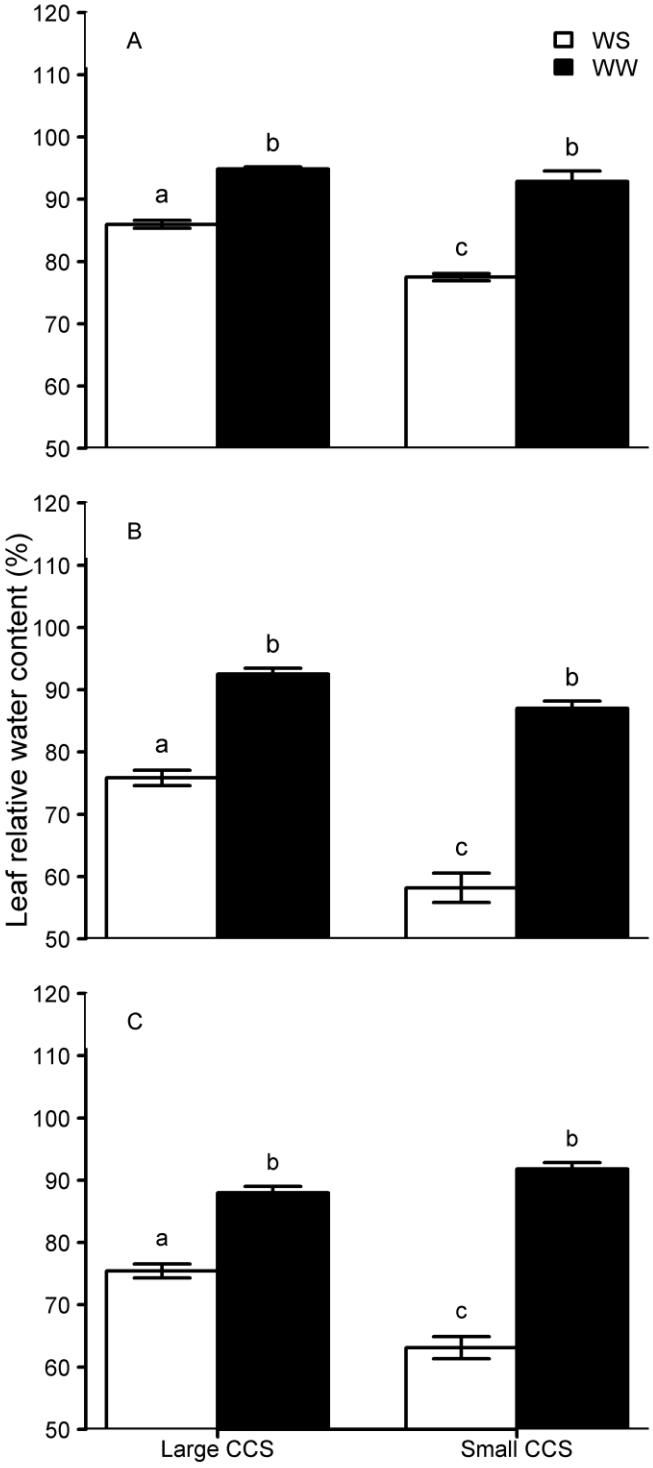

Figure 6. Leaf relative water content for genotypes with large and small cortical cells at 60 days after planting (DAP) in the field **(A)** PA2011, **(B)** PA2012 and **(C)** MW2012-2 both in well-watered **(WW)** and water-stressed **(WS)** conditions. Data shown are means ± SE of the means for three lines per group (n = 4). Means with the same letters are not significantly different ($p < 0.05$).

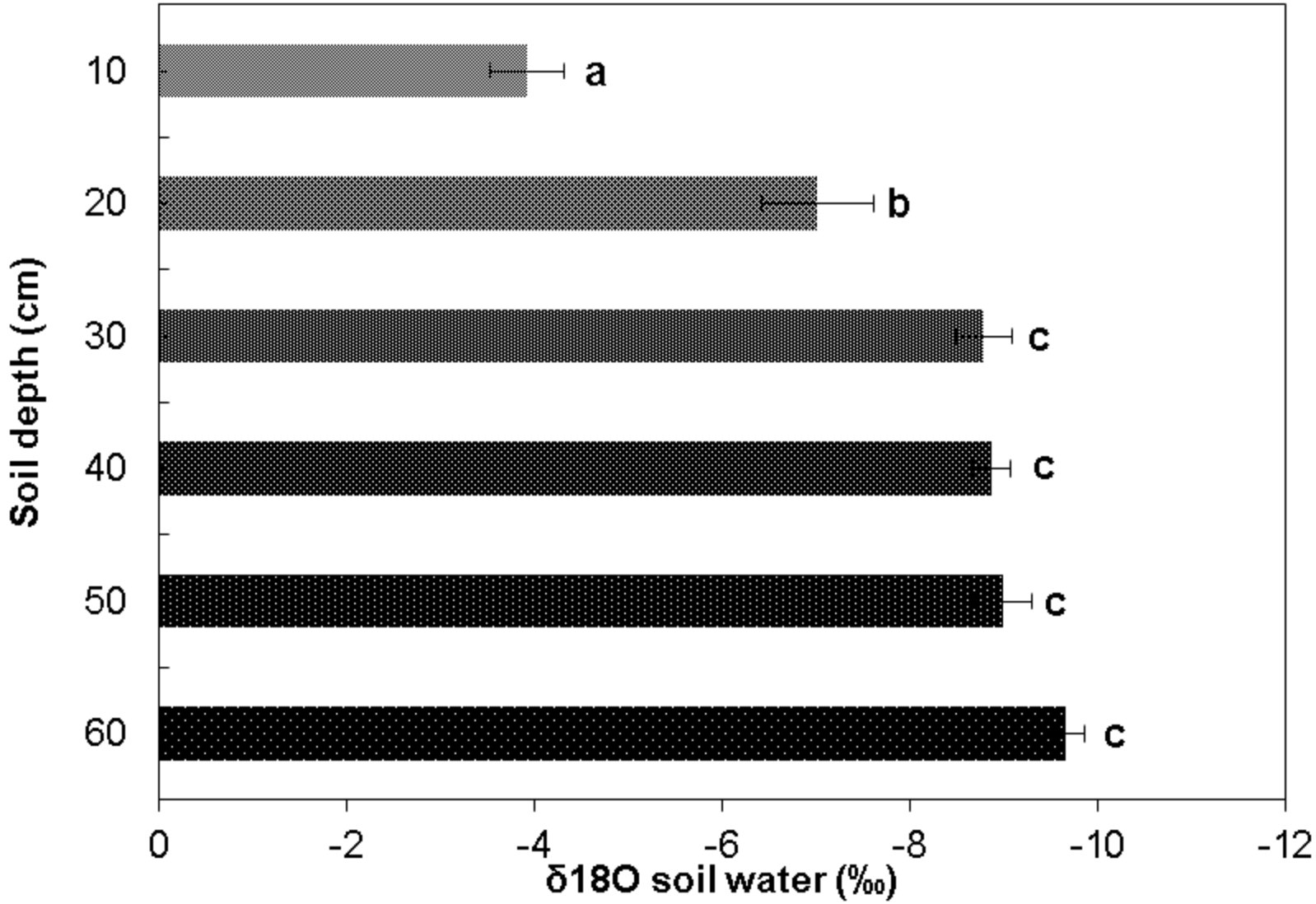

Figure 7. Soil water oxygen isotope composition ± S.E. in six soil layers in the rainout shelters (PA2011). Sampling was done 65 days after planting. Values are the means ±SE of 3 observation points in the rainout shelters.

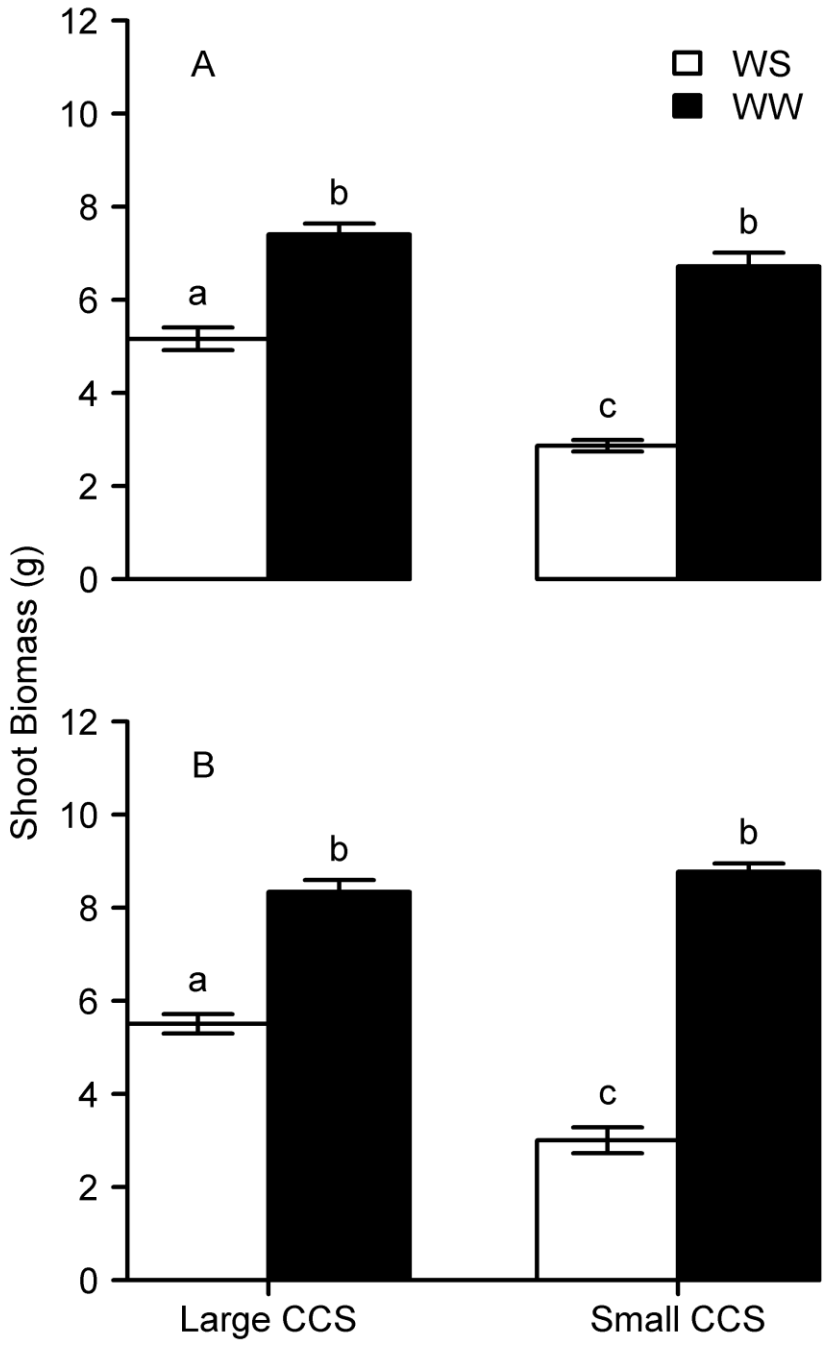

Figure 8. Shoot biomass for genotypes with large and small cortical cells in the mesocosms 30 days after planting **(A)**GH2 and **(B)**GH3 in the mesocosms both in well-watered **(WW)** and water-stressed **(WS)** conditions. Data shown are means ± SE of the means for three lines per group (n = 4). Means with the same letters are not significantly different ($p < 0.05$).

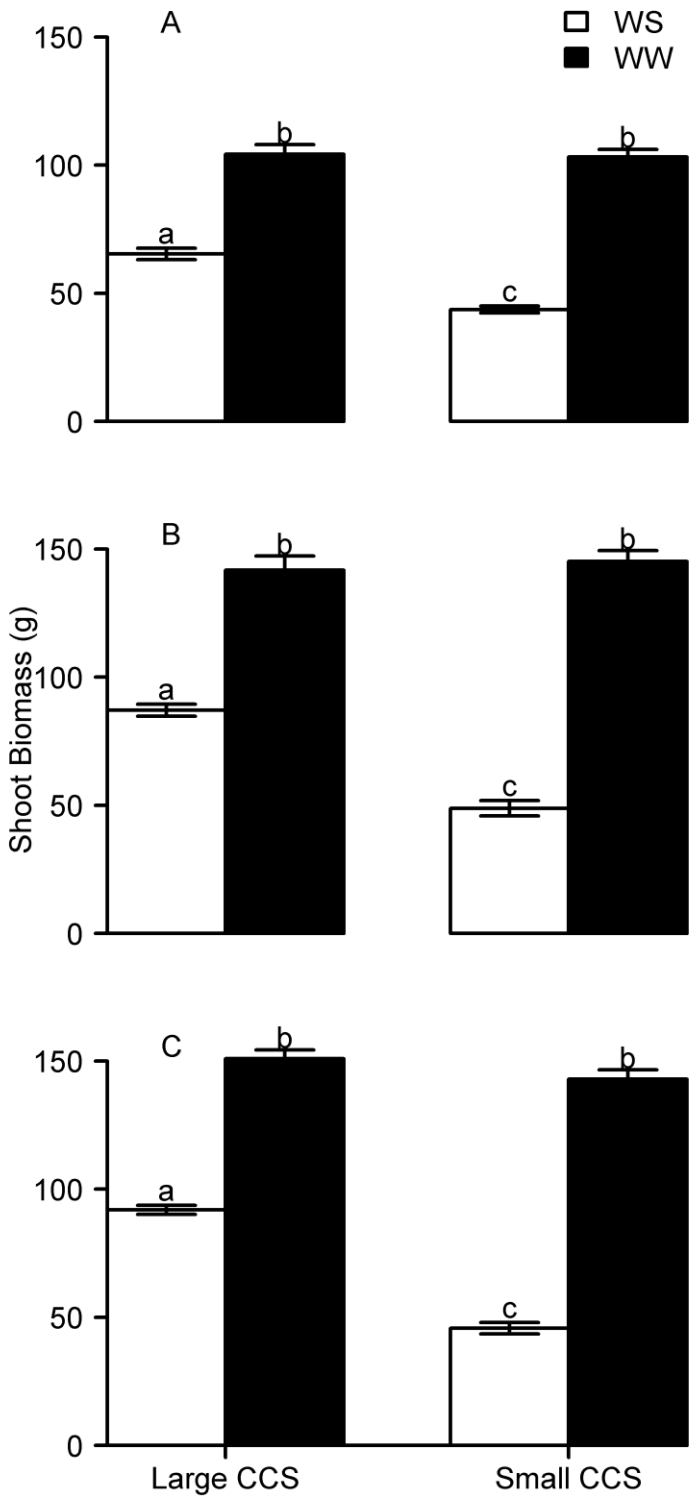

Figure 9. Shoot biomass for genotypes with large and small cortical cells in the field 70 days after planting **(A)** PA2011, **(B)** 2012, and **(C)** MW2012-2 both water-stressed (WS) and well-watered (WW) conditions. Data shown are means ± SE of the means for three lines per group (n = 4). Means with the same letters are not significantly different ($p < 0.05$).

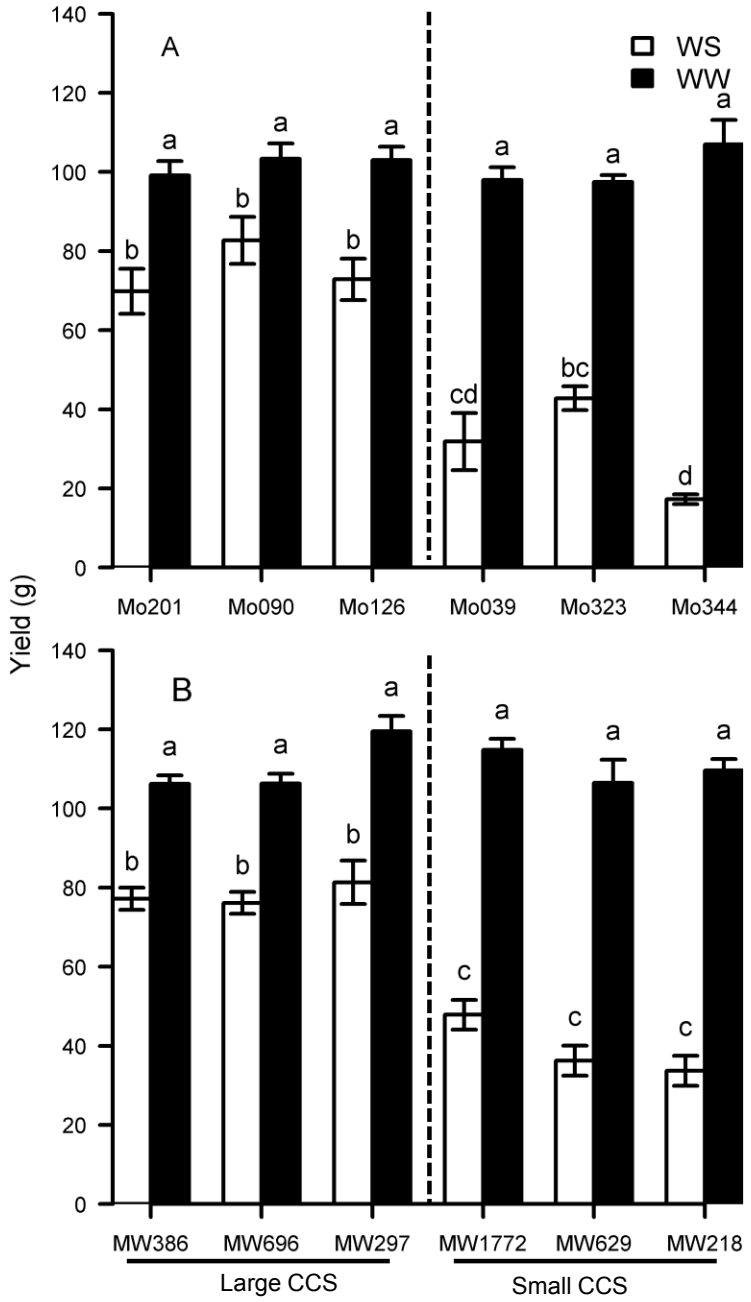

Figure 10. Grain yield for genotypes with large and small cortical cells in the field **(A)** PA2012 and **(B)** MW2012-2 both water-stressed (WS) and well-watered (WW) conditions. Data shown are means ± SE of the means (n = 4). Means with the same letters are not significantly different ($p < 0.05$).

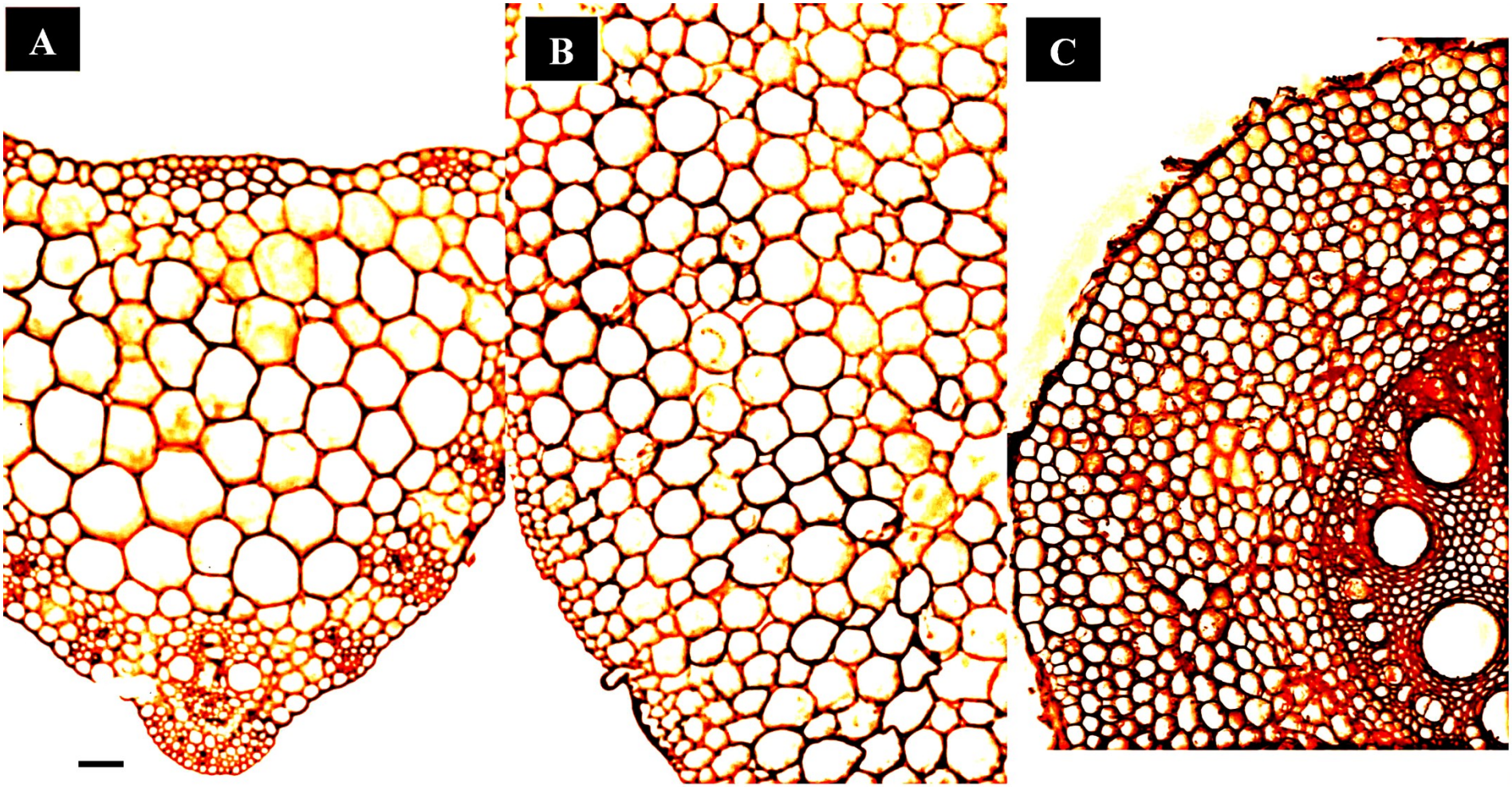

Supplemental Figure S1. Transverse section showing parenchyma cells in maize for (A) leaf midrib, (B) mesocotyl cortex and (C) root cortex for the same plant. The black scale bar in bottom left represents 100 microns in length. The images were obtained using laser ablation tomography.

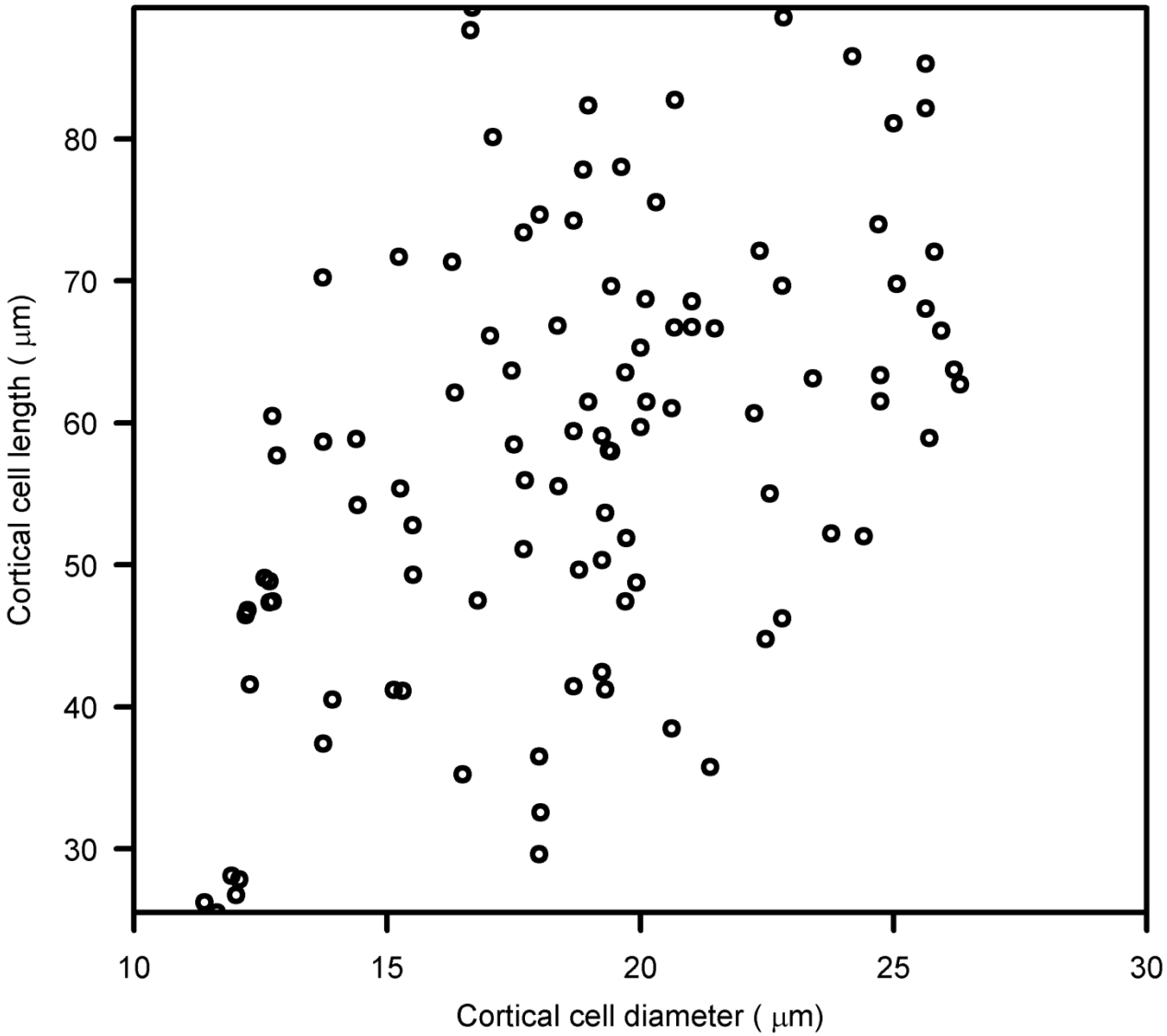

Supplemental Figure S2. Correlation between cortical cell diameter and cell length ($y = 1.802x + 24.313$, $R^2 = 0.2309$)

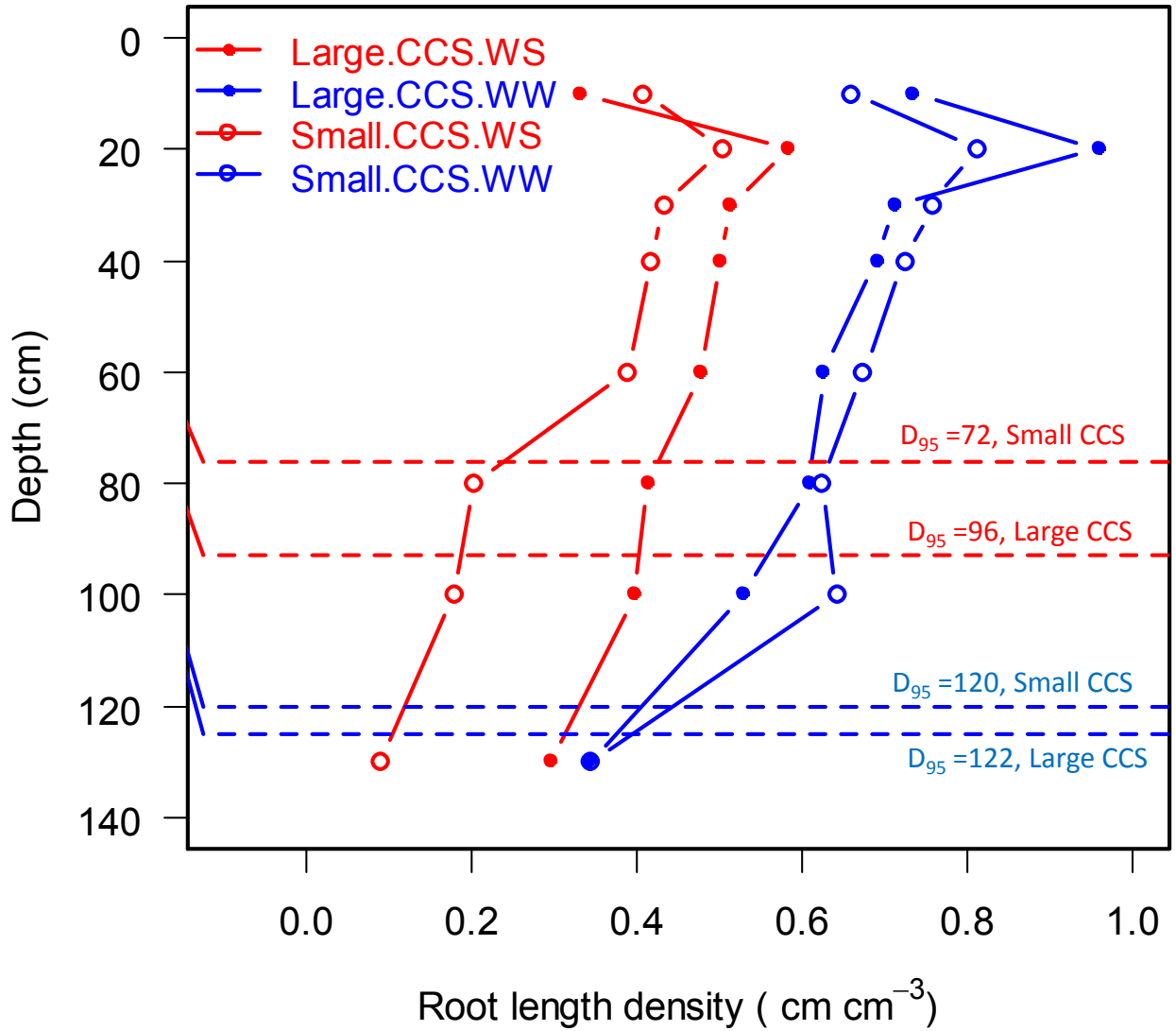

Supplemental Figure S3. Root length density at different soil depths for genotypes with large CCS and small CCS under water stressed (WS) and well watered (WW) conditions in the greenhouse (GH1) with corresponding D_{95}. D_{95} measures the depth above where 95% of root length is present.

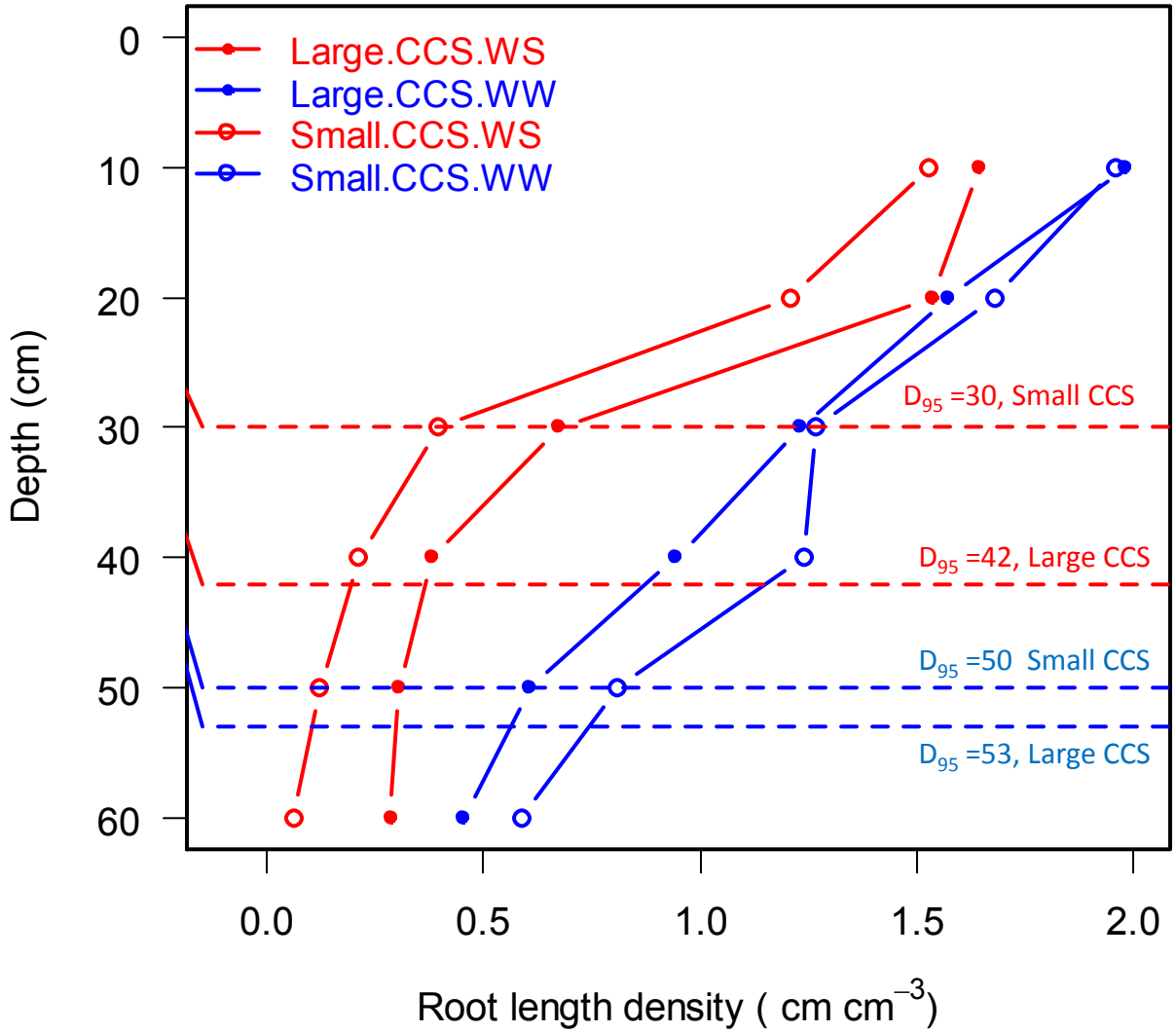

Supplemental Figure S4. Root length density at different soil depths for genotypes with large CCS and small CCS under water stressed (WS) and well watered (WW) conditions in the field (PA2011) with corresponding D_{95}. D_{95} measures the depth above where 95% of root length is present.

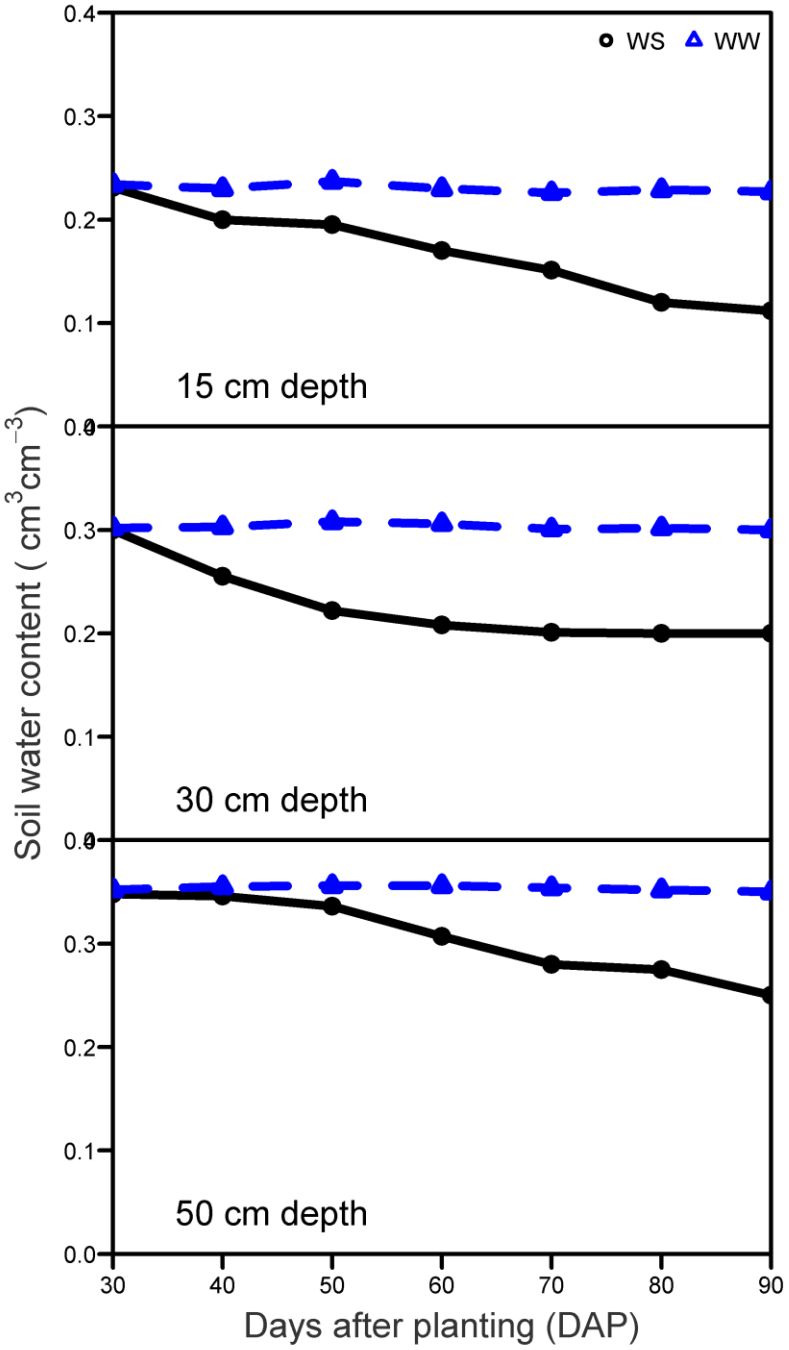

Supplemental Figure S5. Change in soil moisture content at different depths (15cm, 30cm, and 50cm) in well watered (WW) and water stressed (WS) plots for PA2012. Terminal drought was imposed in WS plots beginning at 30 DAP.